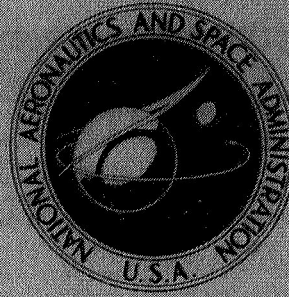


N71-22622

**NASA TECHNICAL  
MEMORANDUM**



NASA TM X-2261

NASA TM X-2261

**CASE FILE  
COPY**

**SUBSONIC AERODYNAMIC CHARACTERISTICS OF  
A HIGHLY SWEEP FIXED-WING CONFIGURATION  
WITH VARIATION IN WING-DIHEDRAL ANGLE**

*by William P. Henderson*

*Langley Research Center*

*Hampton, Va. 23365*

NATIONAL AERONAUTICS AND SPACE ADMINISTRATION • WASHINGTON, D. C. • APRIL 1971

1. Report No. NASA TM X-2261		2. Government Accession No.		3. Recipient's Catalog No.	
4. Title and Subtitle SUBSONIC AERODYNAMIC CHARACTERISTICS OF A HIGHLY SWEEP FIXED-WING CONFIGURATION WITH VARIATION IN WING-DIHEDRAL ANGLE				5. Report Date April 1971	
				6. Performing Organization Code	
7. Author(s) William P. Henderson				8. Performing Organization Report No. L-7473	
9. Performing Organization Name and Address  NASA Langley Research Center Hampton, Va. 23365				10. Work Unit No. 720-01-10-01	
				11. Contract or Grant No. *	
12. Sponsoring Agency Name and Address  National Aeronautics and Space Administration Washington, D.C. 20546				13. Type of Report and Period Covered Technical Memorandum	
				14. Sponsoring Agency Code	
15. Supplementary Notes					
16. Abstract  <p>An investigation to determine the effects of wing-dihedral angle on the aerodynamic characteristics of a highly swept fixed-wing configuration was conducted in the Langley high-speed 7- by 10-foot tunnel. The tests were conducted at a Mach number of 0.168, at angles of attack of <math>-5^{\circ}</math> to <math>22^{\circ}</math>, and at sideslip angles of <math>0^{\circ}</math> and <math>\pm 5^{\circ}</math>. The effects of the addition of vertical tails, vertical-tail cant angle, and leading-edge flap deflection on the aerodynamic characteristics are also included.</p>					
17. Key Words (Suggested by Author(s))  Subsonic speeds Wing-dihedral angle Highly swept fixed wing Lateral stability				18. Distribution Statement  Unclassified -- Unlimited	
19. Security Classif. (of this report) Unclassified		20. Security Classif. (of this page) Unclassified		21. No. of Pages 44	
				22. Price* \$3.00	

SUBSONIC AERODYNAMIC CHARACTERISTICS  
OF A HIGHLY SWEPT FIXED-WING CONFIGURATION  
WITH VARIATION IN WING-DIHEDRAL ANGLE

By William P. Henderson  
Langley Research Center

SUMMARY

An investigation to determine the effects of wing-dihedral angle on the aerodynamic characteristics of a highly swept fixed-wing configuration was conducted in the Langley high-speed 7- by 10-foot tunnel. The tests were conducted at a Mach number of 0.168, at angles of attack of  $-5^{\circ}$  to  $22^{\circ}$ , and at sideslip angles of  $0^{\circ}$  and  $\pm 5^{\circ}$ . The effects of the addition of vertical tails, vertical-tail cant angle, and leading-edge flap deflection on the aerodynamic characteristics are also included.

The data indicate that the addition of the vertical tails results in improvements in the static stability characteristics (instability delayed to higher lift coefficient), a directionally stable configuration throughout the angle-of-attack range, and a slight reduction in the effective-dihedral parameters. Canting the vertical tails significantly reduces the directional stability and slightly increases the effective-dihedral parameter at the higher angles of attack. Deflecting the leading-edge flaps results in fairly large improvements in the longitudinal static stability characteristics, reduces the drag due to lift, and gives an unstable increment in directional stability at intermediate angles of attack. Varying the geometric-dihedral angle in the wing at the various spanwise locations in such a manner that the vertical position of the wing tip remains unchanged relative to the horizontal reference plane has only a slight effect on the aerodynamic characteristics. Varying the wing dihedral, with no consideration as to the location of the wing tip with respect to the horizontal reference plane (which means that some of the deflections studied are too extreme to incorporate into a transport configuration), has only a slight effect on the longitudinal characteristics but results in large changes in the effective-dihedral parameter.

INTRODUCTION

The National Aeronautics and Space Administration has been studying the aerodynamic characteristics of a number of configurations which may be suitable for a supersonic commercial air transport (SCAT). The majority of the results are summarized in reference 1.

One of the more promising configurations, designated SCAT 15-F, has undergone a significant development program, and some of the results are presented in references 2 to 5. One of the aerodynamic problems related to this type of highly swept, low-aspect-ratio wing configuration is the high level of rolling moment due to sideslip angle exhibited at moderate and high angles of attack. Excessive amounts of rolling moment due to sideslip may place strenuous design requirements on the lateral-control system in order to assure satisfactory handling qualities under conditions of crosswind landing and lateral gust. One method of reducing the rolling moment due to sideslip is by incorporating negative geometric dihedral into the wing design. The purpose of this paper is to present the results of a study in which the geometric-dihedral angle was varied at several spanwise stations. The study was conducted in the Langley high-speed 7- by 10-foot tunnel at a Mach number of 0.168 through an angle-of-attack range of  $-5^\circ$  to  $22^\circ$  and at sideslip angles of  $0^\circ$  and  $\pm 5^\circ$ .

## SYMBOLS

The data presented herein are referred to the body-axis system, with the exception of lift and drag coefficients, which are referred to the wind-axis system. All the data are referred to a moment center located at fuselage station 159.28 cm.

b	reference wing span, 111.658 cm
$\bar{c}$	mean geometric chord, 94.213 cm
$C_D$	drag coefficient, $\frac{\text{Drag}}{qS}$
$C_l$	rolling-moment coefficient, $\frac{\text{Rolling moment}}{qSb}$
$C_{l_\beta}$	effective-dihedral parameter, $\frac{C_{l_{(\beta=5^\circ)}} - C_{l_{(\beta=-5^\circ)}}}{\Delta\beta}$ , per deg
$C_{l_{\beta\Gamma}}$	variation of effective-dihedral parameter with dihedral angle
$C_L$	lift coefficient, $\frac{\text{Lift}}{qS}$
$C_m$	pitching-moment coefficient, $\frac{\text{Pitching moment}}{qS\bar{c}}$
$C_n$	yawing-moment coefficient, $\frac{\text{Yawing moment}}{qSb}$

$C_{n\beta}$	directional-stability parameter, $\frac{C_{n(\beta=50)} - C_{n(\beta=-50)}}{\Delta\beta}$ , per deg
$C_Y$	side-force coefficient, $\frac{\text{Side force}}{qS}$
$C_{Y\beta}$	side-force parameter, $\frac{C_{Y(\beta=50)} - C_{Y(\beta=-50)}}{\Delta\beta}$ , per deg
$q$	dynamic pressure, N/m <sup>2</sup>
$S$	wing area, 7599.34 cm <sup>2</sup>
$y$	spanwise distance from plane of symmetry, cm
$\alpha$	angle of attack, deg
$\beta$	angle of sideslip, deg
$\Gamma_B$	wing geometric-dihedral angle, deg
$\Gamma_{B1}$	wing geometric-dihedral angle at break 1, deg (positive outboard tip up)
$\Gamma_{B2}$	wing geometric-dihedral angle at break 2, deg (positive outboard tip up)
$\Gamma_{B3}$	wing geometric-dihedral angle at break 3, deg (positive outboard tip up)
$\delta_n$	leading-edge flap deflections, deg (positive leading edge up)
$\delta_v$	vertical-tail cant angle, deg (positive tip inboard)

Designation:

$V_t$  vertical tails

## MODEL

A three-view drawing of the model configuration studied during this investigation is shown in figure 1(a). This configuration employs a highly sweptback fixed wing with a cranked tip. The wing had a flat airfoil section with beveled leading and trailing edges; it had a constant thickness of 1.59 cm from the wing root out to the wing-leading-edge

break. Outboard of this break the thickness varied from 1.59 cm to 0.795 cm at the wing tip. The wing incorporated a 15-percent-chord leading-edge flap which extended from 15.7 percent of the wing semispan to about 73.1 percent of the wing semispan.

Three break locations, about which the wing dihedral could be varied, were incorporated into the wing. These breaks were located at 15.7, 41.0, and 73.1 percent of the wing semispan. As indicated in figure 1(a) the dihedral angle of any one of the wing sections is always defined relative to the chord plane of the section just inboard of the deflected section. (See fig. 1(b)).

## TEST AND CORRECTIONS

The investigation was conducted in the Langley high-speed 7- by 10-foot tunnel at a Mach number of 0.168, which corresponds to a dynamic pressure of 1943.9 N/m<sup>2</sup> and a Reynolds number, based on  $\bar{c}$ , of  $3.25 \times 10^6$ . The tests were conducted over an angle-of-attack range of  $-5^\circ$  to  $22^\circ$  and at sideslip angles of  $0^\circ$  and  $\pm 5^\circ$ .

In order to insure turbulent flow in the model boundary layer for the test, 0.32-cm-wide transition strips of No. 80 carborundum grains were placed 2.54 cm, measured streamwise, behind the leading edge of the wing and tails.

The angle of attack was corrected for deflection of the sting-support system under load. The drag data were adjusted to correspond to a pressure at the base of the fuselage equal to free-stream static pressure. Jet-boundary and blockage corrections calculated by the methods of references 6 and 7, respectively, have been applied to the data.

## PRESENTATION OF DATA

The results of this investigation are presented in figures 2 to 16. In order to aid in location of a particular set of data, the following outline of figure contents is presented:

	Figure
Effect of vertical tails, $\Gamma_B = 0^\circ$ , $\delta_n = 0^\circ$ . . . . .	2
Effect of vertical-tail cant, $\Gamma_B = 0^\circ$ , $\delta_n = 0^\circ$ . . . . .	3
Effect of geometric dihedral at:	
Break location 1, $\Gamma_{B2} = \Gamma_{B3} = 0^\circ$ , $\delta_n = 0^\circ$ , $V_t$ off . . . . .	4
Break location 2, $\Gamma_{B1} = \Gamma_{B3} = 0^\circ$ , $\delta_n = 0^\circ$ , $V_t$ on . . . . .	5
Break location 2, $\Gamma_{B1} = \Gamma_{B3} = 0^\circ$ , $\delta_n = 0^\circ$ , $V_t$ off . . . . .	6
Break location 3, $\Gamma_{B1} = \Gamma_{B2} = 0^\circ$ , $\delta_n = 0^\circ$ , $V_t$ on . . . . .	7
Break location 3, $\Gamma_{B1} = 0^\circ$ , $\Gamma_{B2} = -5^\circ$ , $\delta_n = 0^\circ$ , $V_t$ off . . . . .	8
Break locations 1, 2, and 3, $\delta_n = 0^\circ$ , $V_t$ off . . . . .	9

	Figure
Effect of leading-edge flaps, $\Gamma_B = 0^\circ$ , $V_t$ off . . . . .	10
Effect of vertical tails, $\delta_n = -30^\circ$ , $\Gamma_{B1} = \Gamma_{B2} = 0^\circ$ , $\Gamma_{B3} = -10^\circ$ . . . . .	11
Effect of geometric-dihedral angle at break location 3 with	
$\Gamma_{B1} = \Gamma_{B2} = 0^\circ$ , $\delta_n = -30^\circ$ , $V_t$ off . . . . .	12
$\Gamma_{B1} = 0^\circ$ , $\Gamma_{B2} = -5^\circ$ , $\delta_n = -30^\circ$ , $V_t$ off . . . . .	13
$\Gamma_{B1} = 0^\circ$ , $\Gamma_{B2} = -10^\circ$ , $\delta_n = -30^\circ$ , $V_t$ off . . . . .	14
Effect of geometric dihedral at all break locations	
$\delta_n = -30^\circ$ , $V_t$ off . . . . .	15
Variation of the effective-dihedral parameter with geometric-dihedral angle placed at various spanwise locations . . . . .	16

## DISCUSSION OF GEOMETRIC EFFECTS

### Effect of Vertical Tails

The data presented in figure 2 for the configuration with zero wing dihedral show that the vertical tails have a beneficial effect on the longitudinal aerodynamic characteristics. The vertical tails, acting as wing fences, improve the flow characteristics outboard of the vertical tails and result in improved static stability characteristics (instability delayed to higher lift coefficient) and lower drag due to lift as illustrated in figure 2(a).

The lateral directional stability characteristics, presented in figure 2(b), indicate that the wing-body configuration exhibits positive dihedral effect ( $-C_{l_\beta}$ ) and directional instability throughout the test angle-of-attack range.

Adding the vertical tails to the configuration slightly reduced  $C_{l_\beta}$  over most of the test angle-of-attack range and resulted in a directionally stable configuration. The directional stability ( $C_{n_\beta}$ ) is seen to increase sharply at angles of attack above about  $6.5^\circ$  (fig. 2(b)). This increase is probably associated with favorable sidewash angles produced by the wing-body vortices.

Canting the vertical tails (inboard), as shown by the data presented in figure 3(a), results in improvement in the variation of pitching-moment coefficient with lift coefficient. This improvement results from an interaction of the wing-body vortex system with the vertical tails. Figure 3(b) shows that canting the vertical tail significantly alters the directional stability characteristics at the higher angles of attack. It would appear

that canting the vertical tails places them in a rather unfavorable location with respect to the wing-body vortices. Canting the vertical tails also slightly increases the effective-dihedral parameter ( $C_{l_\beta}$ ) at the higher angles of attack (fig. 3(b)).

### Effect of Wing Dihedral

Varying the wing-dihedral angle at each of the three wing-break locations (see figs. 4, 6, and 8 for the configuration with vertical tails off) only slightly affected the longitudinal and lateral stability characteristics.

The effects of wing-dihedral angle on the effective-dihedral parameter ( $C_{l_\beta}$ ) as presented in figures 4, 6, and 8 are summarized in figure 16, and show, as would be expected, that as the break line is moved outboard the increment in  $C_{l_\beta}$  per degree of wing-dihedral angle decreases significantly. This figure also illustrates an interesting angle-of-attack effect on  $C_{l_\beta}$  for the various wing-break locations, in that the increment in  $C_{l_\beta}$  increases with angle of attack for wing-break location 3 and decreases at the other two break locations.

Varying the wing-dihedral angle at wing-break location 2 for the configuration with the vertical tails on results in a slightly larger effect on  $C_{l_\beta}$  than for the configuration without the vertical tails (compare figs. 5(b) and 6(b)). This effect can probably be attributed to vertical-tail cant, since the vertical tails were fixed with respect to the wing, and wing-dihedral changes also produce vertical-tail cant.

Figure 9 presents the effects of various configurations of geometric wing dihedral on the aerodynamic characteristics of the wing-body configuration. The combinations of dihedral angles presented in these figures were chosen so that the height of the wing tip would vary less than 2.54 cm (model scale) from its original flat-wing position. As indicated in figure 9 varying the geometric dihedral along the wing span in such a manner that the wing tip is in essentially the same location has only a slight effect on the aerodynamic characteristics, with the largest effect appearing in the pitching-moment variation with lift coefficient.

### Effect of Leading-Edge Flaps

The effect of leading-edge flap deflection on the aerodynamic characteristics of the configuration is presented in figure 10. Fairly large improvements in the longitudinal static stability and drag characteristics (fig. 10(a)) are evident as a result of the effective wing camber (reducing leading-edge separation) produced by leading-edge flap deflection. Deflecting the leading-edge flaps has an adverse effect on the directional stability characteristics of the configuration without the vertical tails (see fig. 10(b)) over most of the angle-of-attack range. In the intermediate angle-of-attack range,  $5^\circ$  to  $15^\circ$ , deflecting the leading-edge flaps results in a destabilizing increment in directional

stability ( $C_{n\beta}$ ) and a positive increment in the side-force parameter ( $C_{Y\beta}$ ). Although these effects are not fully understood, they are believed associated with the alteration of the wing-body vortex system caused by leading-edge flap deflection.

For the configuration with the leading-edge flaps deflected  $-30^\circ$ , the vertical tails had only a slight effect on the longitudinal characteristics (fig. 11(a)); this effect is in contrast to those illustrated in figure 2(a), which shows that for the configuration with the flaps neutral the vertical tails caused a large improvement in the pitching-moment characteristics. As previously suggested, the vertical tails acting as wing fences (flaps neutral condition) shield the outboard wing panels from the wing-body vortex flow field and result in the indicated pitching-moment improvements. Deflecting the leading-edge flaps, however, delays or alters the formation of the leading-edge vortex in such a manner that the vertical tail no longer functions as wing fences and consequently no significant change in the pitching-moment characteristics results.

Adding the vertical tails to the configuration, as illustrated by the data presented in figure 11(b), slightly reduced  $C_{l\beta}$  over the test angle-of-attack range and results in a directionally stable configuration.

The effect of various amounts of geometric-dihedral angle on the aerodynamic characteristics for the configuration with the leading-edge flap deflected  $-30^\circ$  is presented in figures 12 to 15. The deflections studied were chosen without consideration as to the location of the wing tips with respect to the horizontal reference plane. Some of the deflection angles studied are probably too extreme to be incorporated into a possible transport configuration, since ground clearance has to be a major consideration in any design. In general, changing the wing dihedral has only a slight effect on the longitudinal characteristics of the configuration. The lateral characteristics ( $C_{l\beta}$ ) in some cases show significant changes over those for the basic flat wing. For example, at an angle of attack of  $10^\circ$  the basic configurations have a value of  $C_{l\beta}$  of  $-0.0022$  (fig. 2(b)), whereas the various combinations of geometric dihedral studied resulted in as much as a 50-percent reduction in  $C_{l\beta}$ .

## CONCLUSIONS

An investigation to determine the effects of wing-geometric-dihedral angle on the aerodynamic characteristics of a highly swept fixed-wing configuration indicated the following conclusions:

1. The addition of the vertical tails to the wing-body configuration results in improvements in the static stability characteristics (instability delayed to higher lift coefficient), a directionally stable configuration throughout the test angle-of-attack range, and a slight reduction in the effective-dihedral parameters.

2. Canting the vertical tails (tip inboard) significantly reduces the directional stability and slightly increases the effective-dihedral parameter at the higher angles of attack.

3. Deflecting the leading-edge flaps results in fairly large improvements in the longitudinal static stability characteristics, reduces the drag due to lift, and gives an unstable increment in directional stability at intermediate angles of attack.

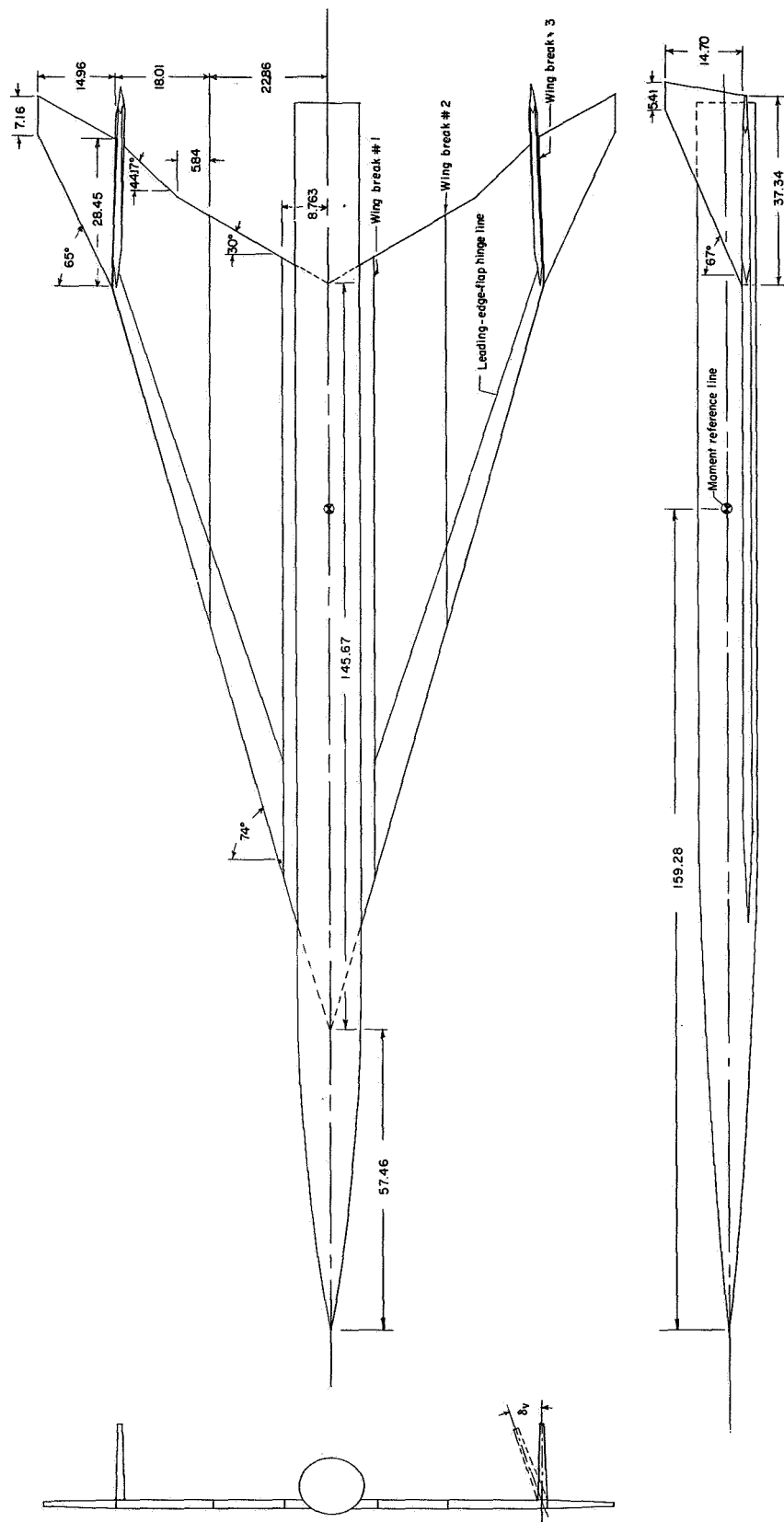
4. Varying the geometric-dihedral angle in the wing at the various spanwise locations in such a manner that the vertical position of the wing tip remains unchanged relative to the horizontal reference plane has only a slight effect on the aerodynamic characteristics of the configuration.

5. Varying the wing dihedral, with no consideration as to the location of the wing tip with respect to the horizontal reference plane (which means that some of the deflections studied are too extreme to incorporate into a transport configuration), has only a slight effect on the longitudinal characteristics, but results in large changes in the effective-dihedral parameter.

Langley Research Center,  
National Aeronautics and Space Administration,  
Hampton, Virginia, February 17, 1971.

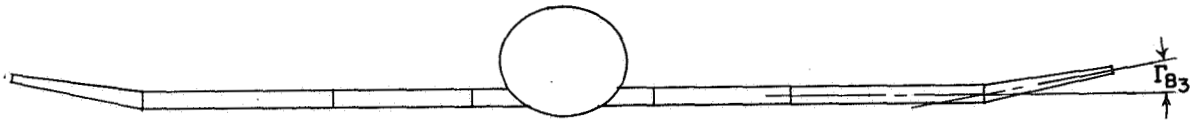
## REFERENCES

1. Ray, Edward J.: NASA Supersonic Commercial Air Transport (SCAT) Configurations: A Summary and Index of Experimental Characteristics. NASA TM X-1329, 1967.
2. Henderson, William P.: Low-Speed Aerodynamic Characteristics of a Supersonic Transport Model With a Highly Swept, Twisted and Combined, Fixed Wing. NASA TM X-1249, 1966.
3. Freeman, Delma C., Jr.: Low Subsonic Flight and Force Investigation of a Supersonic Transport Model With a Highly Swept Arrow Wing. NASA TN D-3887, 1967.
4. Morris, Odell A.; and Fournier, Roger H.: Aerodynamic Characteristics at Mach Numbers 2.30, 2.60, and 2.96 of a Supersonic Transport Model Having a Fixed, Warped Wing. NASA TM X-1115, 1965.
5. Ray, Edward J.; and Henderson, William P.: Low-Speed Aerodynamic Characteristics of a Highly Swept Supersonic Transport Model With Auxiliary Canard and High-Lift Devices. NASA TM X-1694, 1968.
6. Gillis, Clarence L.; Polhamus, Edward C.; and Gray, Joseph L., Jr.: Charts For Determining Jet-Boundary Corrections for Complete Models in 7- by 10-Foot Closed Rectangular Wind Tunnels. NACA WR L-123, 1945. (Formerly NACA ARR L5G31.)
7. Herriot, John G.: Blockage Corrections for Three-Dimensional-Flow Closed-Throat Wind Tunnels, With Consideration of the Effect of Compressibility. NACA Rep. 995, 1950. (Supersedes NACA RM A7B28.)

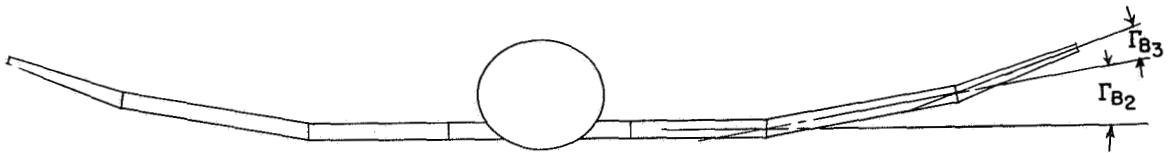


(a) Three views.

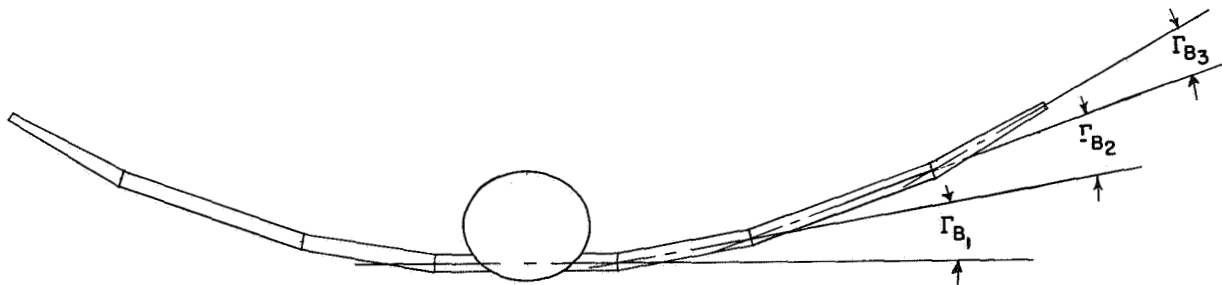
Figure 1.- Drawing of model. (All dimensions in centimeters.)



Dihedral angle for outboard wing panel



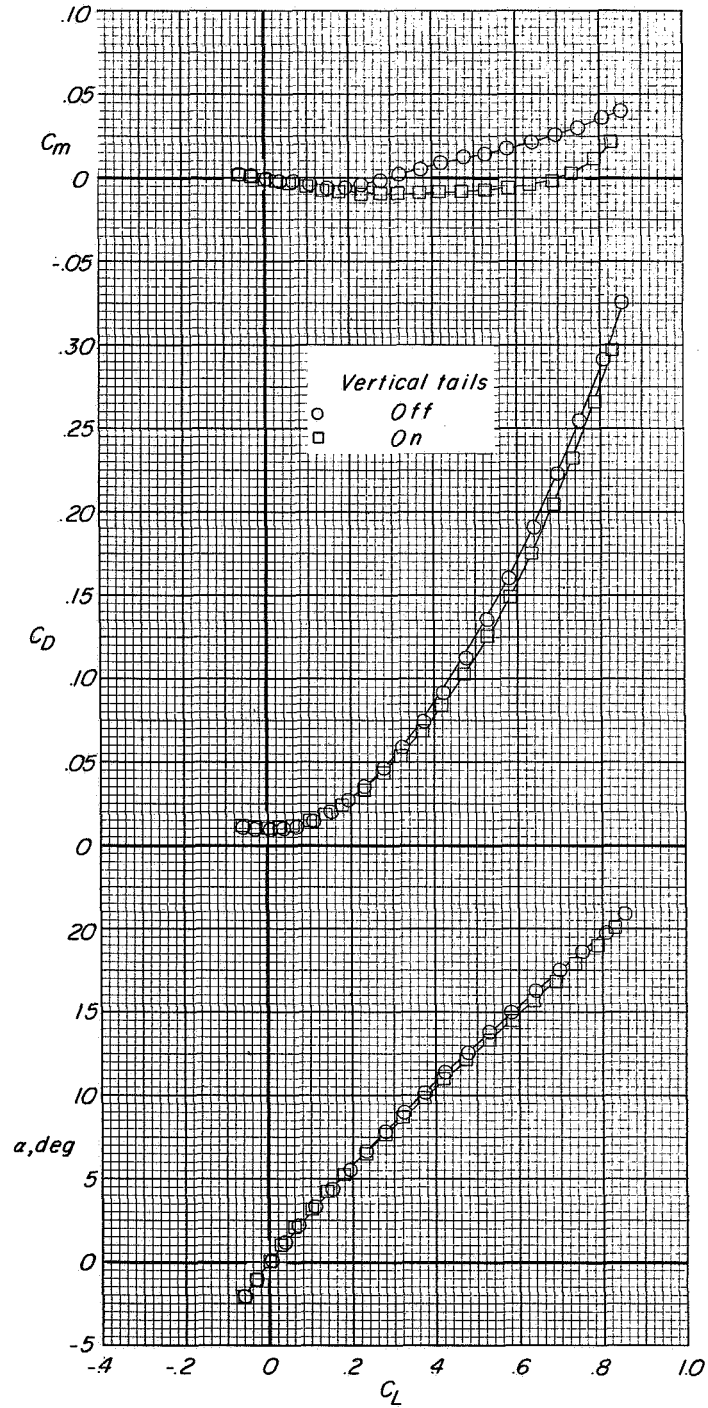
Dihedral angle for intermediate and outboard panels



Dihedral angle for three wing stations

(b) Definition of wing-dihedral angles.

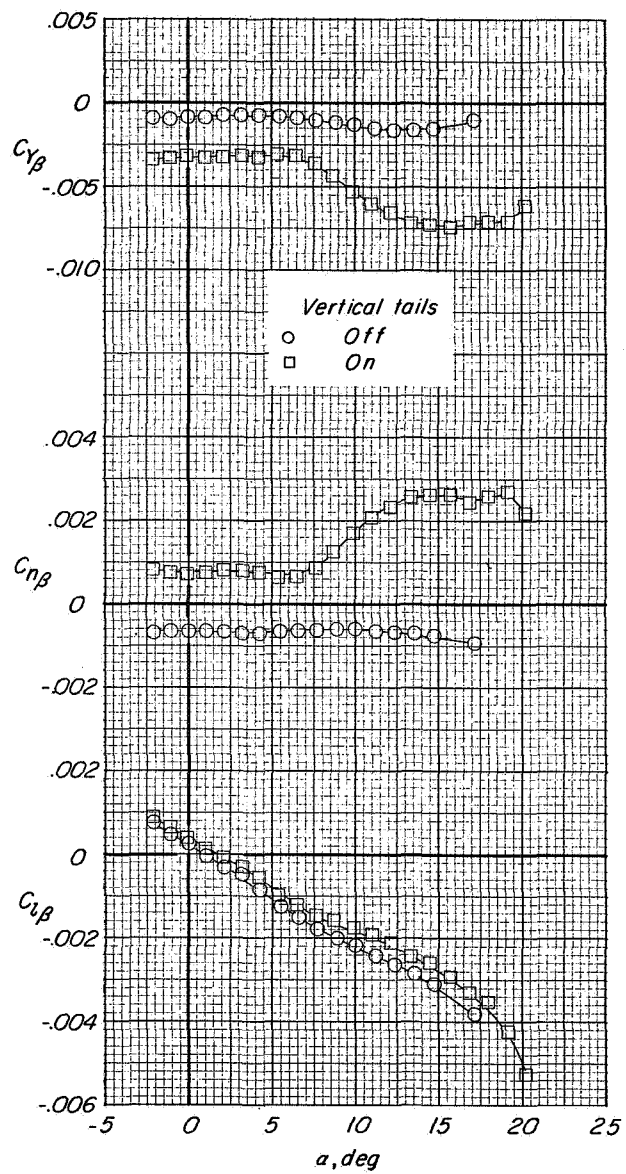
Figure 1.- Concluded.



(a) Longitudinal characteristics.

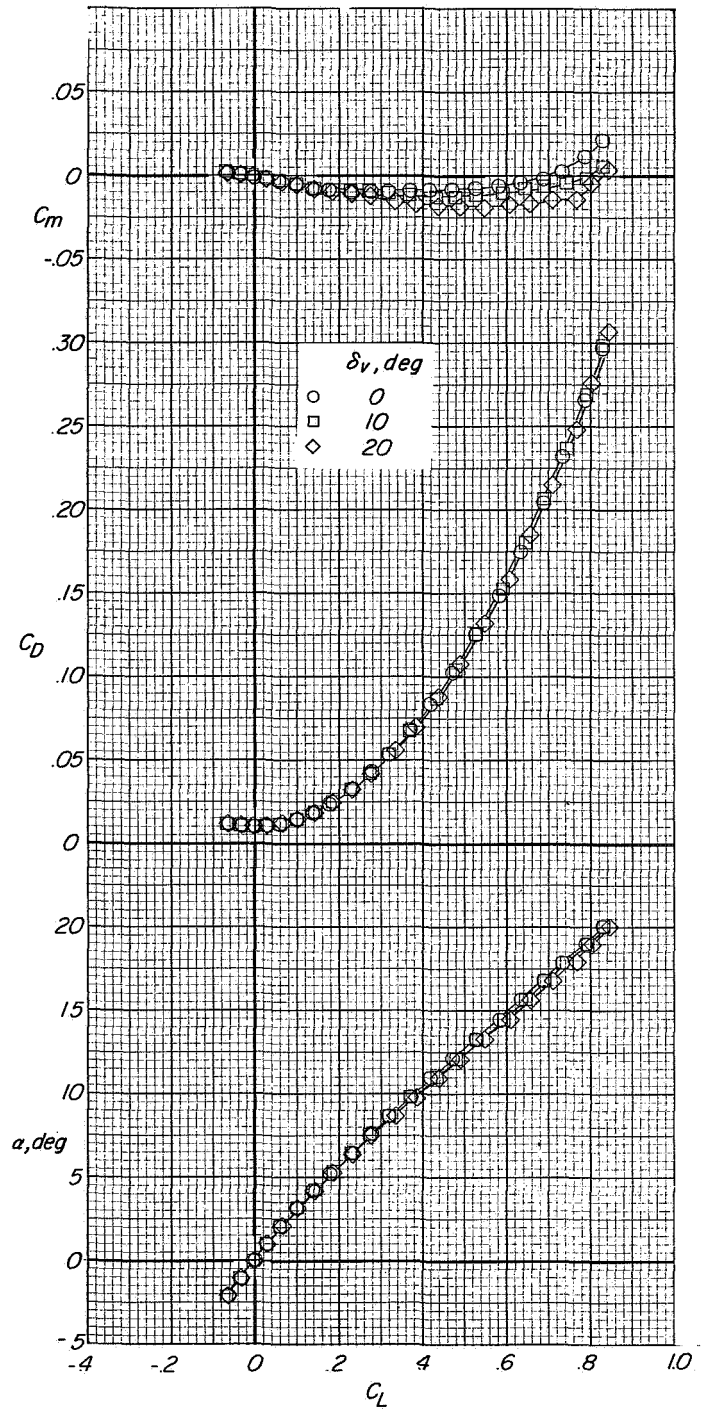
Figure 2.- Effect of vertical tails on aerodynamic characteristics.

$$\Gamma_B = 0^\circ; \quad \delta_n = 0^\circ.$$



(b) Lateral directional characteristics.

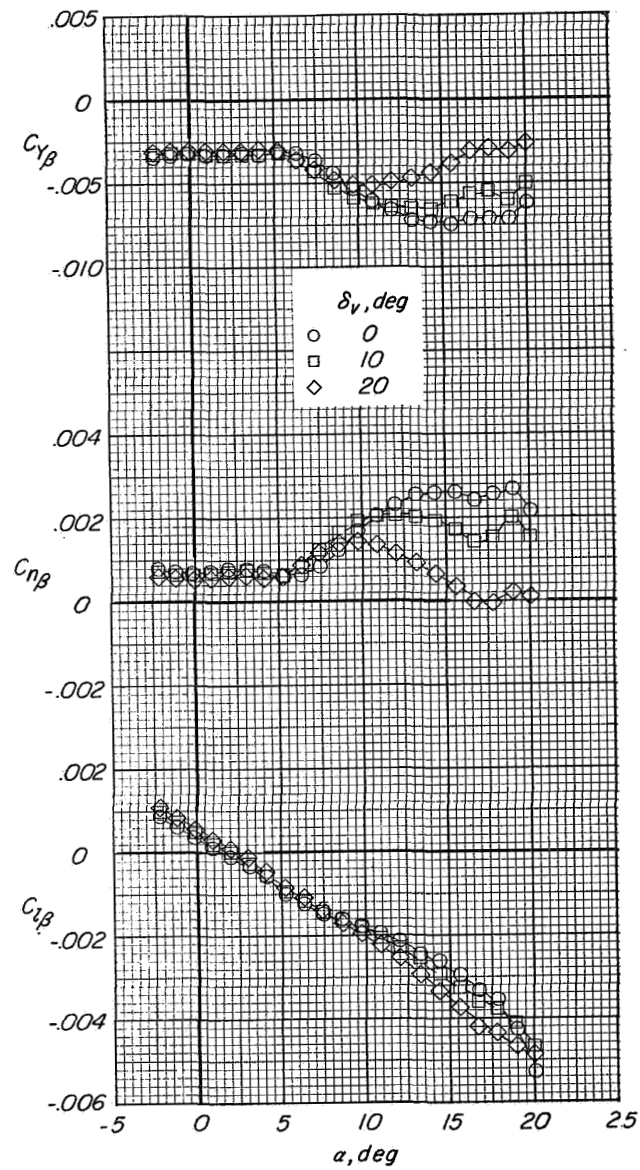
Figure 2.- Concluded.



(a) Longitudinal characteristics.

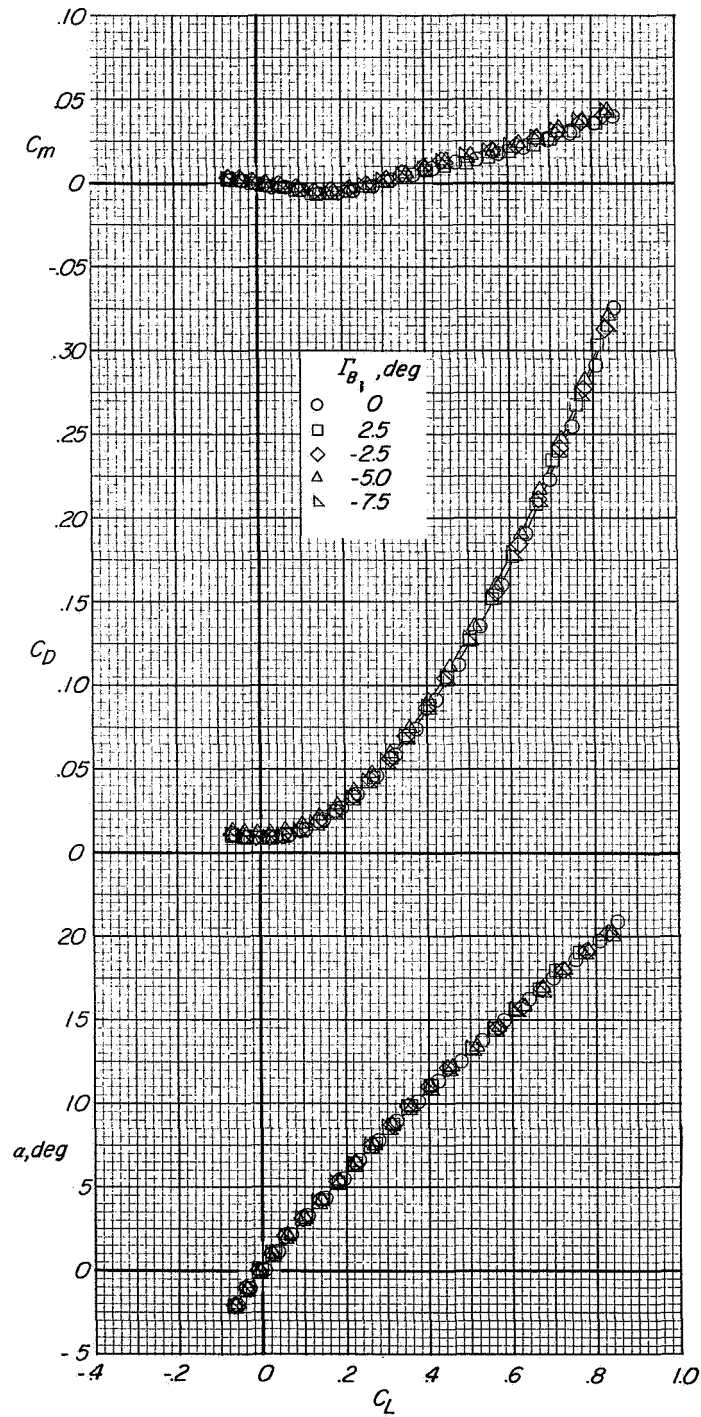
Figure 3.- Effect of vertical-tail cant angle on aerodynamic characteristics.

$$\Gamma_B = 0^\circ; \quad \delta_n = 0^\circ.$$



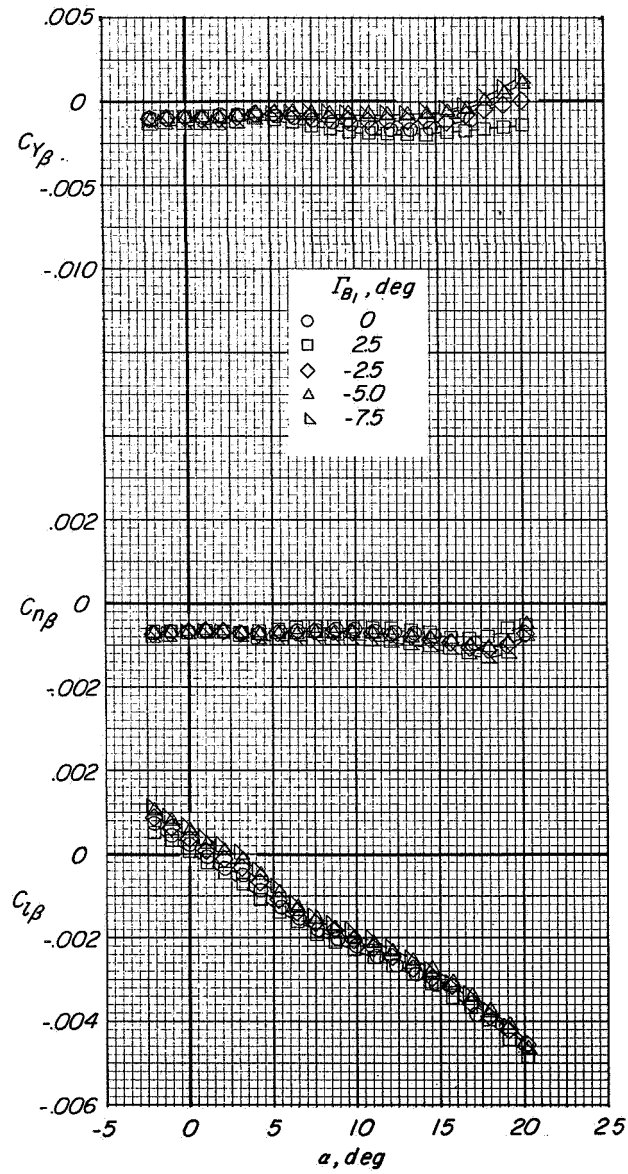
(b) Lateral directional characteristics.

Figure 3.- Concluded.



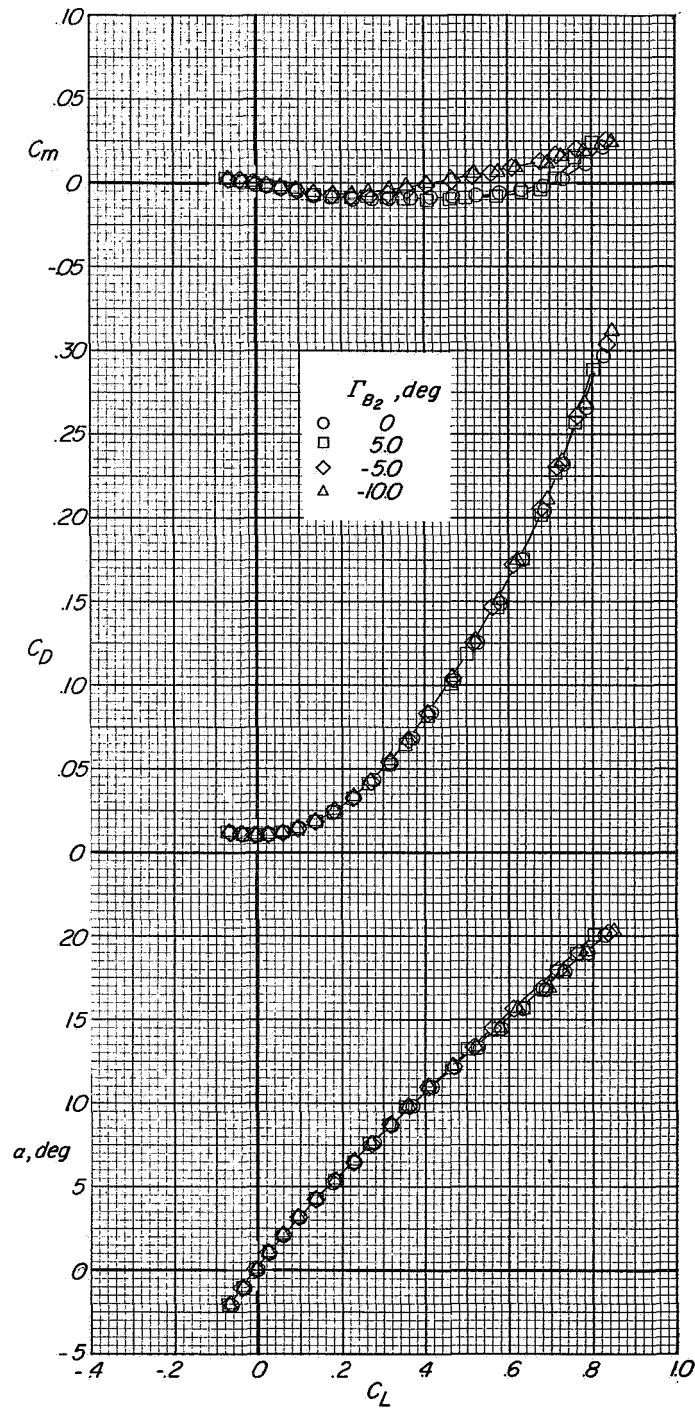
(a) Longitudinal characteristics.

Figure 4.- Effect of geometric dihedral at wing-break location 1 on aerodynamic characteristics.  $\Gamma_{B_2} = 0^\circ$ ;  $\Gamma_{B_3} = 0^\circ$ ;  $\delta_n = 0^\circ$ ;  $V_t$  off.



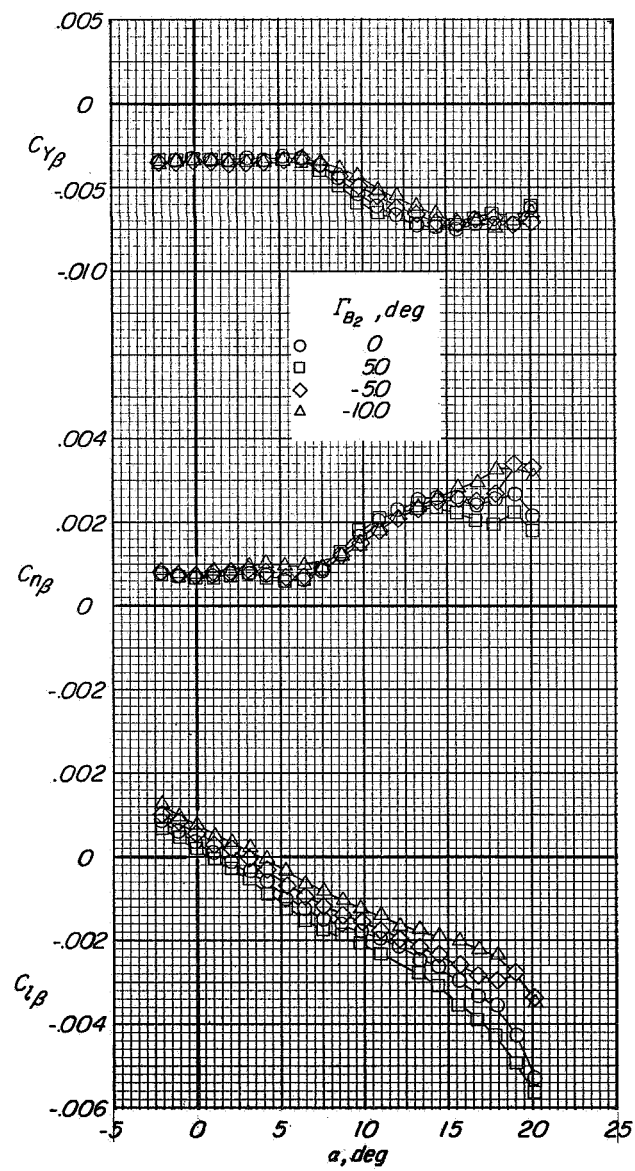
(b) Lateral directional characteristics.

Figure 4.- Concluded.



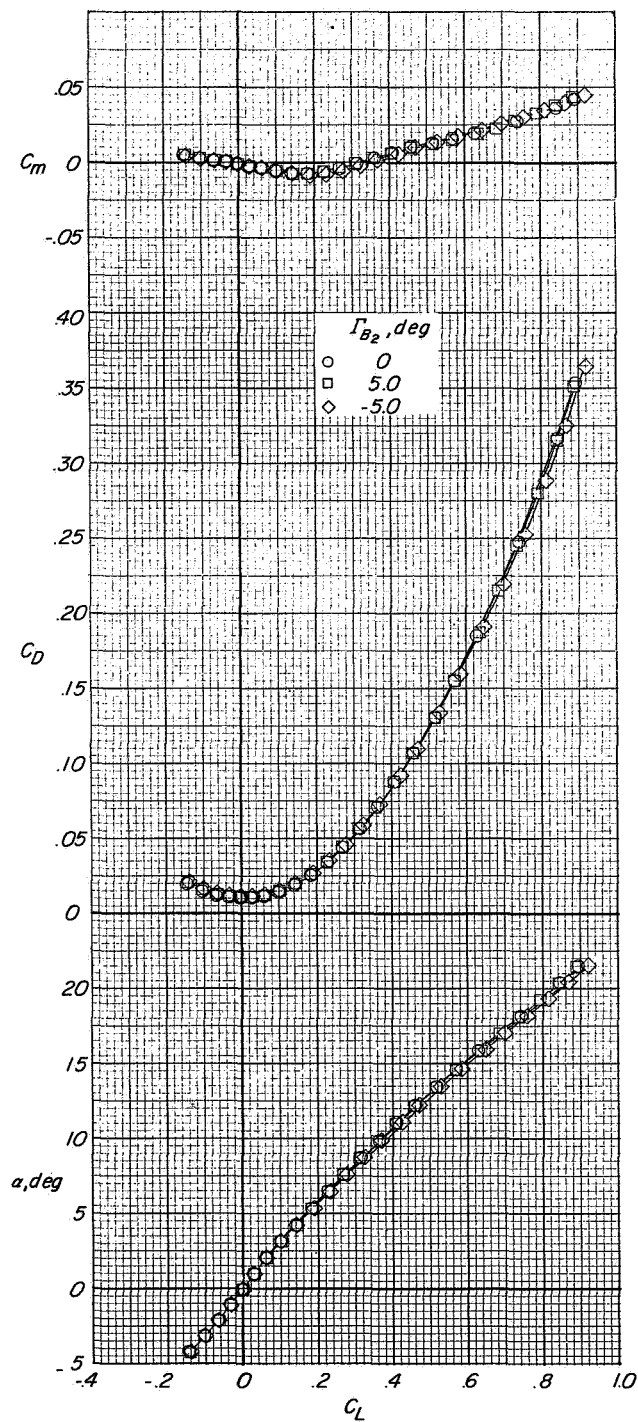
(a) Longitudinal characteristics.

Figure 5.- Effect of geometric dihedral at wing-break location 2 on aerodynamic characteristics of configuration with vertical tails on.  $\Gamma_{B_1} = 0^\circ$ ;  $\Gamma_{B_3} = 0^\circ$ ;  $\delta_n = 0^\circ$ .



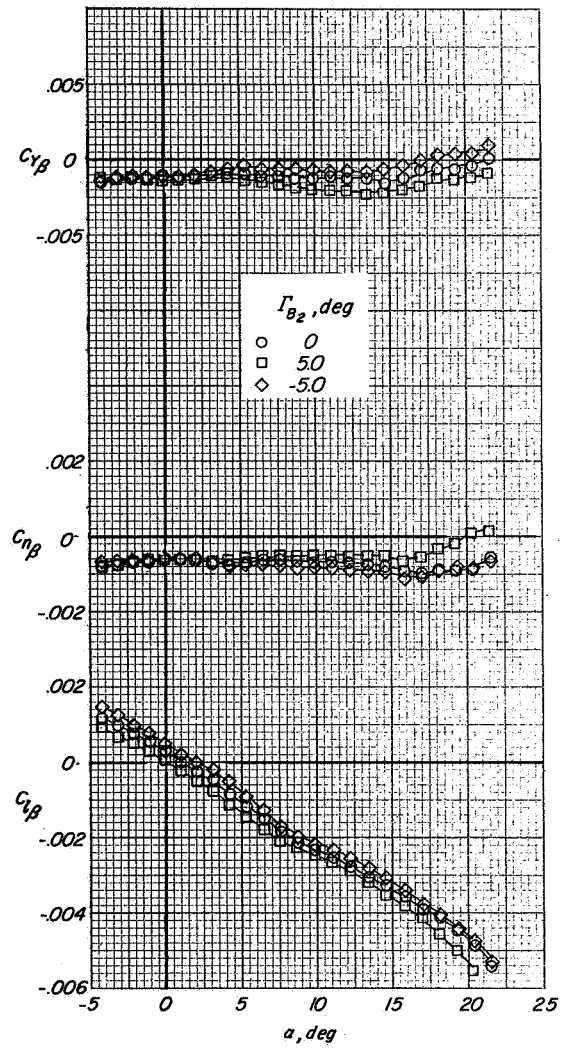
(b) Lateral-directional characteristics.

Figure 5.- Concluded.



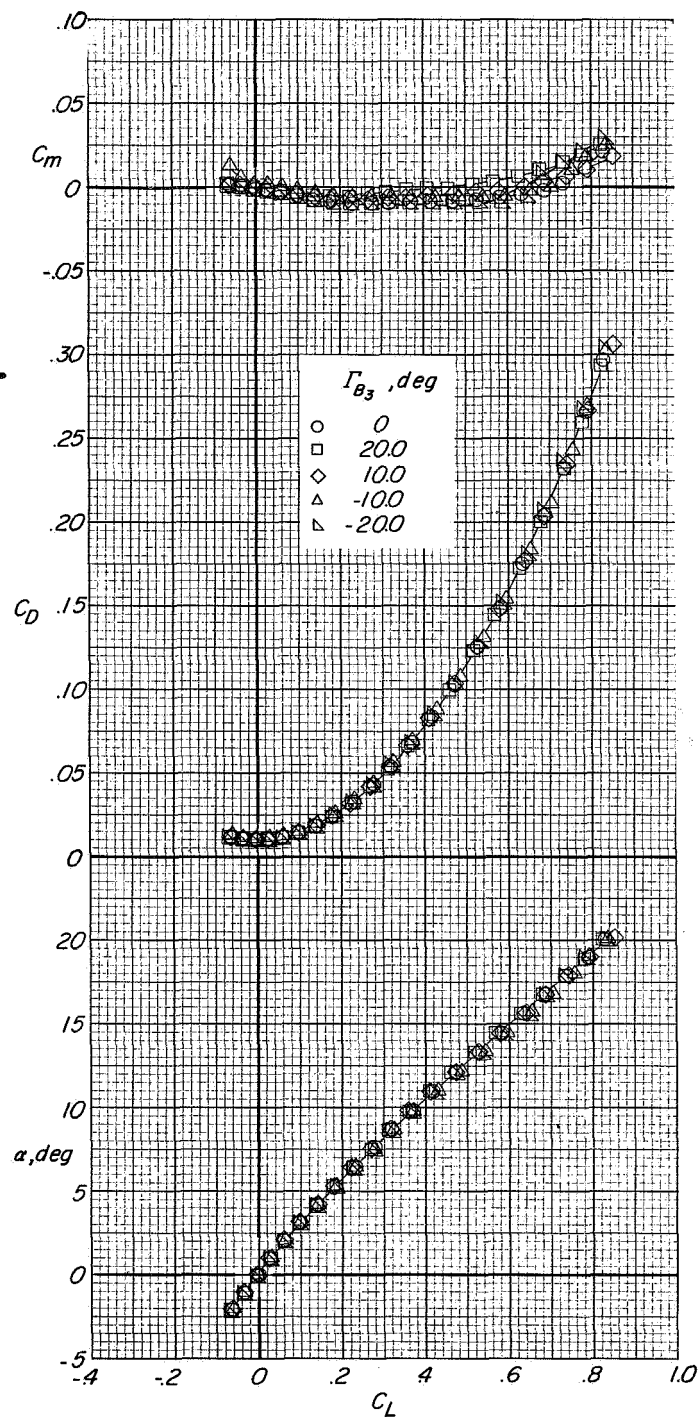
(a) Longitudinal characteristics.

Figure 6.- Effect of geometric dihedral at wing-break location 2 on aerodynamic characteristics of configuration with vertical tails off.  $\Gamma_{B_1} = 0^\circ$ ;  $\Gamma_{B_3} = 0^\circ$ ;  $\delta_n = 0^\circ$ .



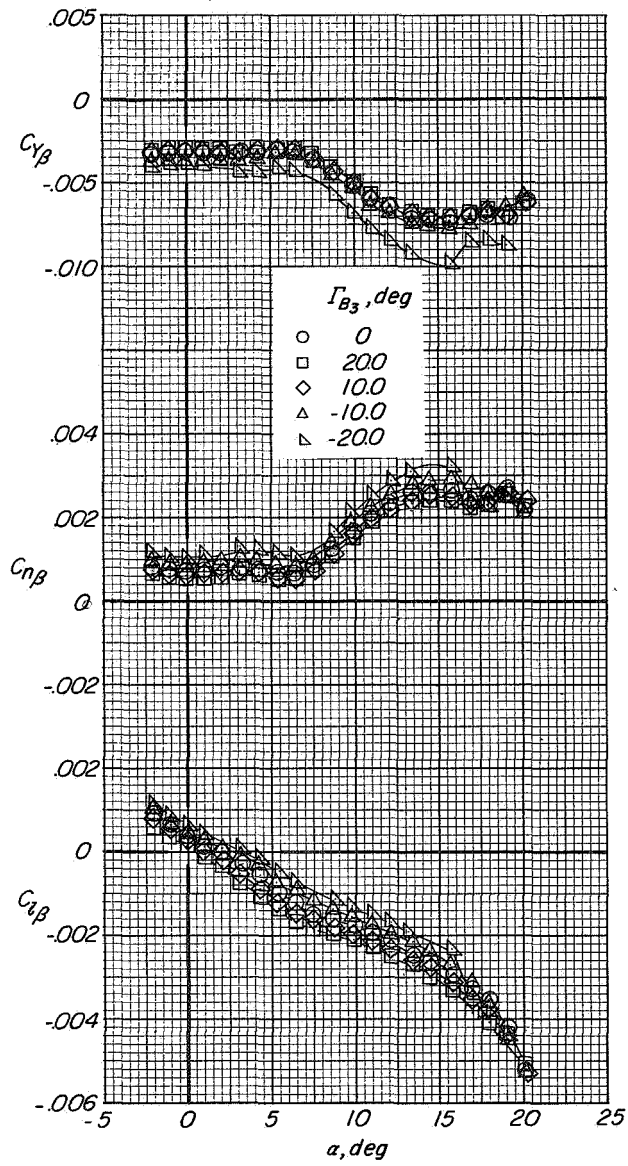
(b) Lateral directional characteristics.

Figure 6.- Concluded.



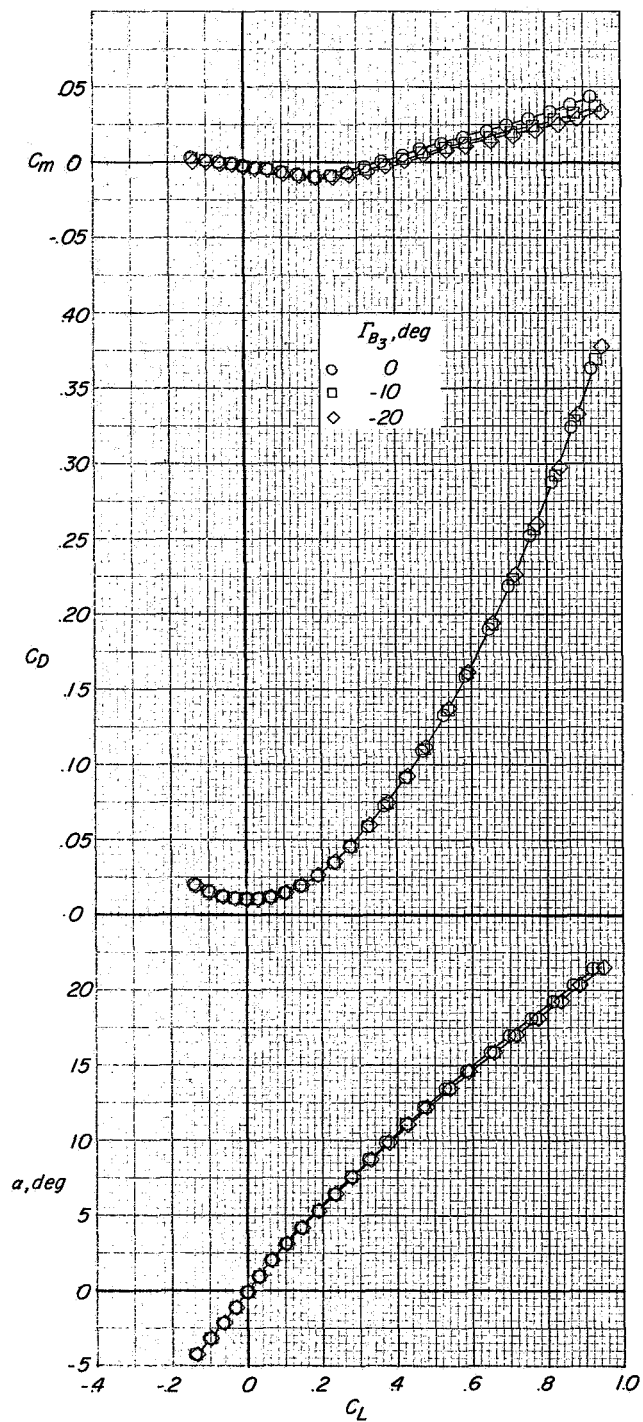
(a) Longitudinal characteristics.

Figure 7.- Effect of geometric dihedral at wing-break location 3 on aerodynamic characteristics.  $\Gamma_{B_1} = 0^\circ$ ;  $\Gamma_{B_2} = 0^\circ$ ;  $\delta_n = 0^\circ$ ;  $V_t$  on.



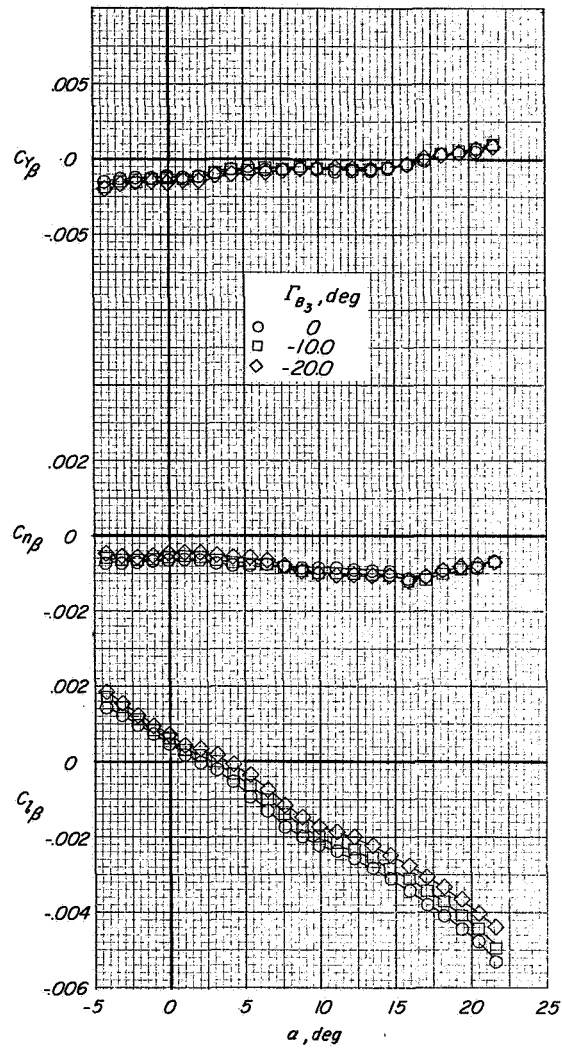
(b) Lateral directional characteristics.

Figure 7.- Concluded.



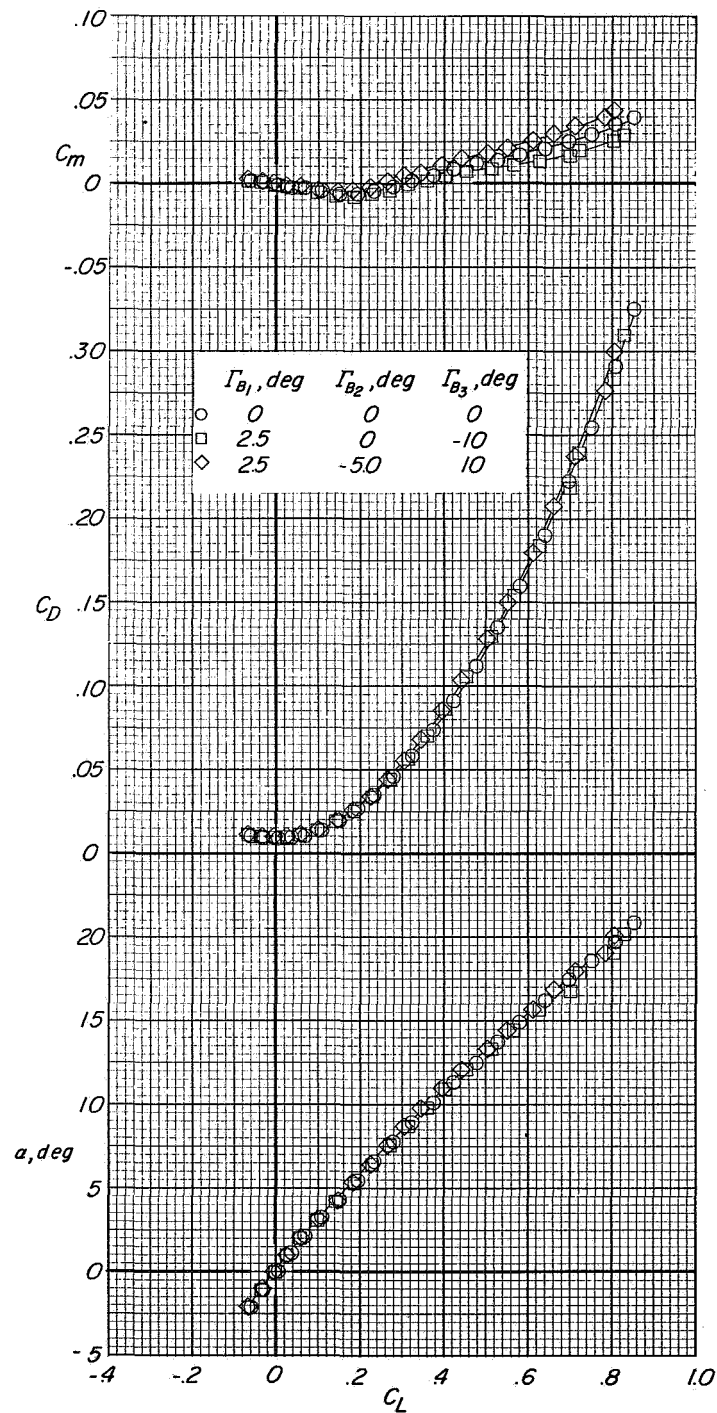
(a) Longitudinal characteristics.

Figure 8.- Effect of geometric dihedral at wing-break location 3 on aerodynamic characteristics.  $\Gamma_{B_1} = 0^\circ$ ;  $\Gamma_{B_2} = -5^\circ$ ;  $\delta_n = 0^\circ$ ;  $V_t$  off.



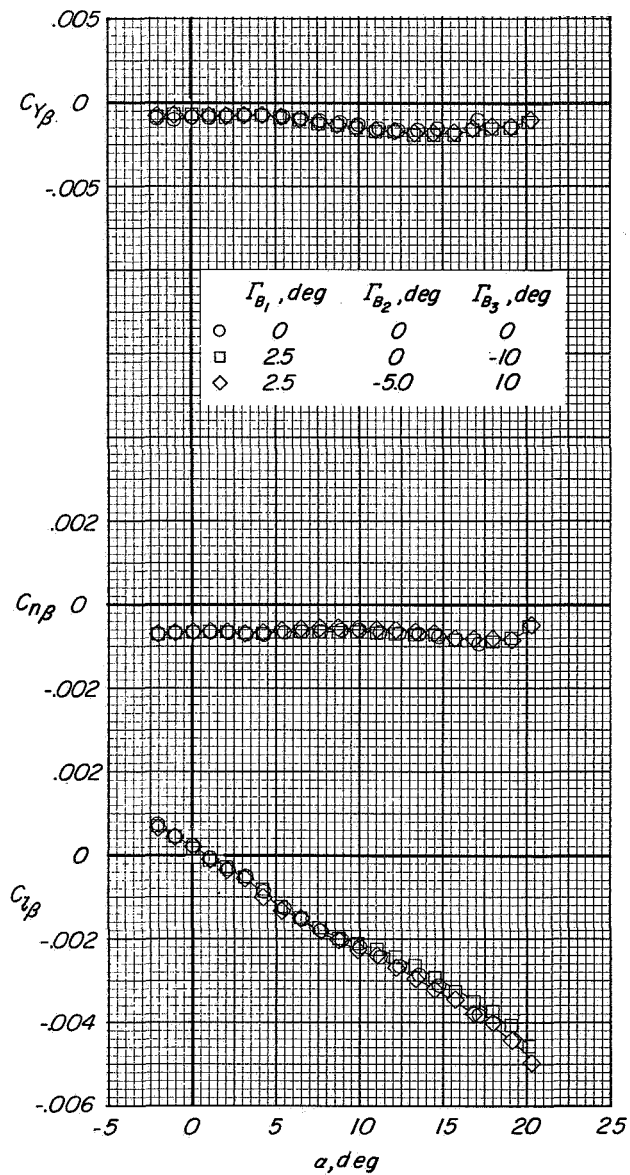
(b) Lateral directional characteristics.

Figure 8.- Concluded.



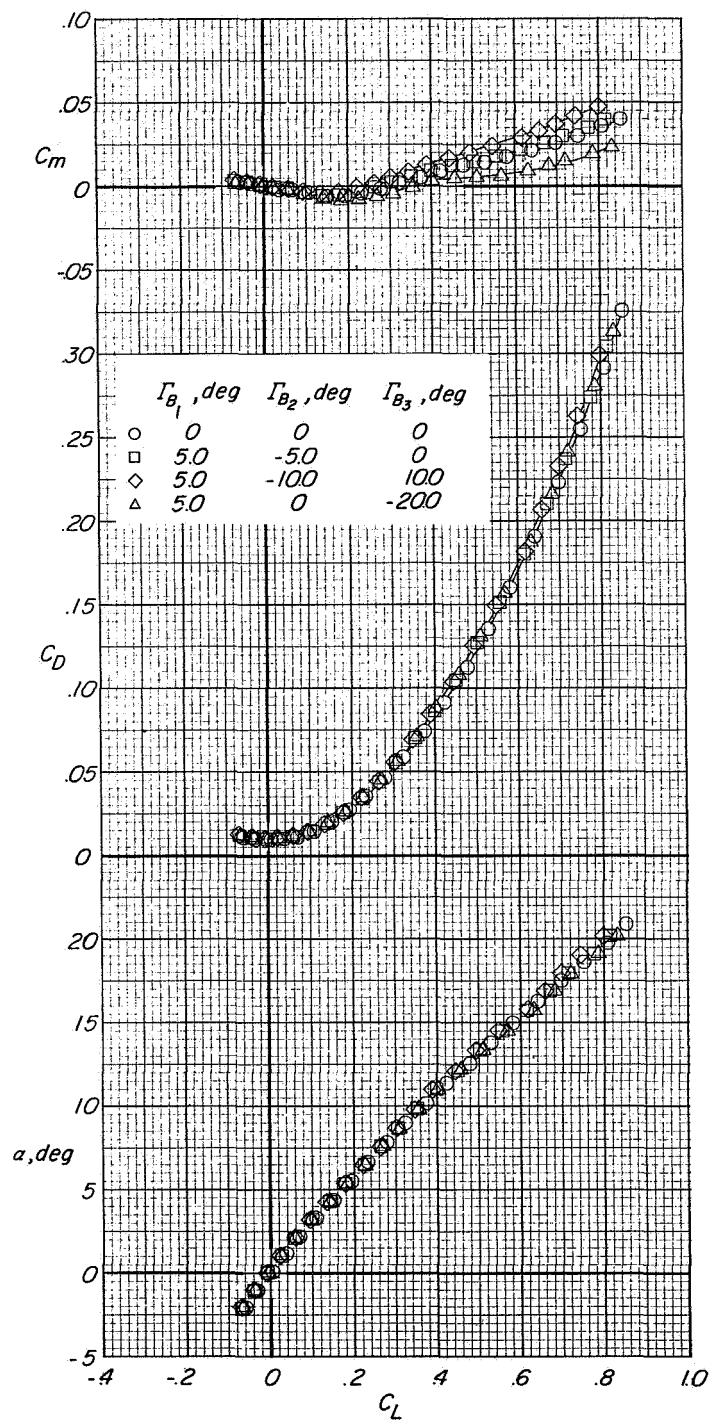
(a) Longitudinal characteristics;  $\Gamma_B = -10^\circ$  to  $10^\circ$ .

Figure 9.- Effect of geometric dihedral angles on aerodynamic characteristics.  $\delta_n = 0^\circ$ ;  $V_t$  off.



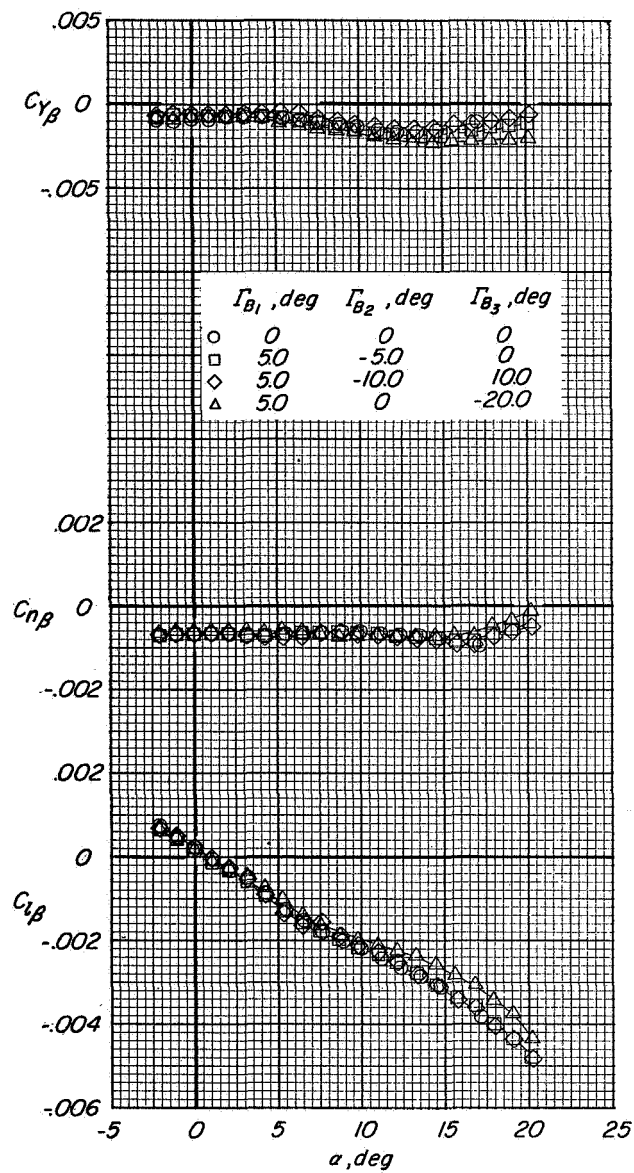
(b) Lateral directional characteristics;  $\Gamma_B = -10^\circ$  to  $10^\circ$ .

Figure 9.- Continued.



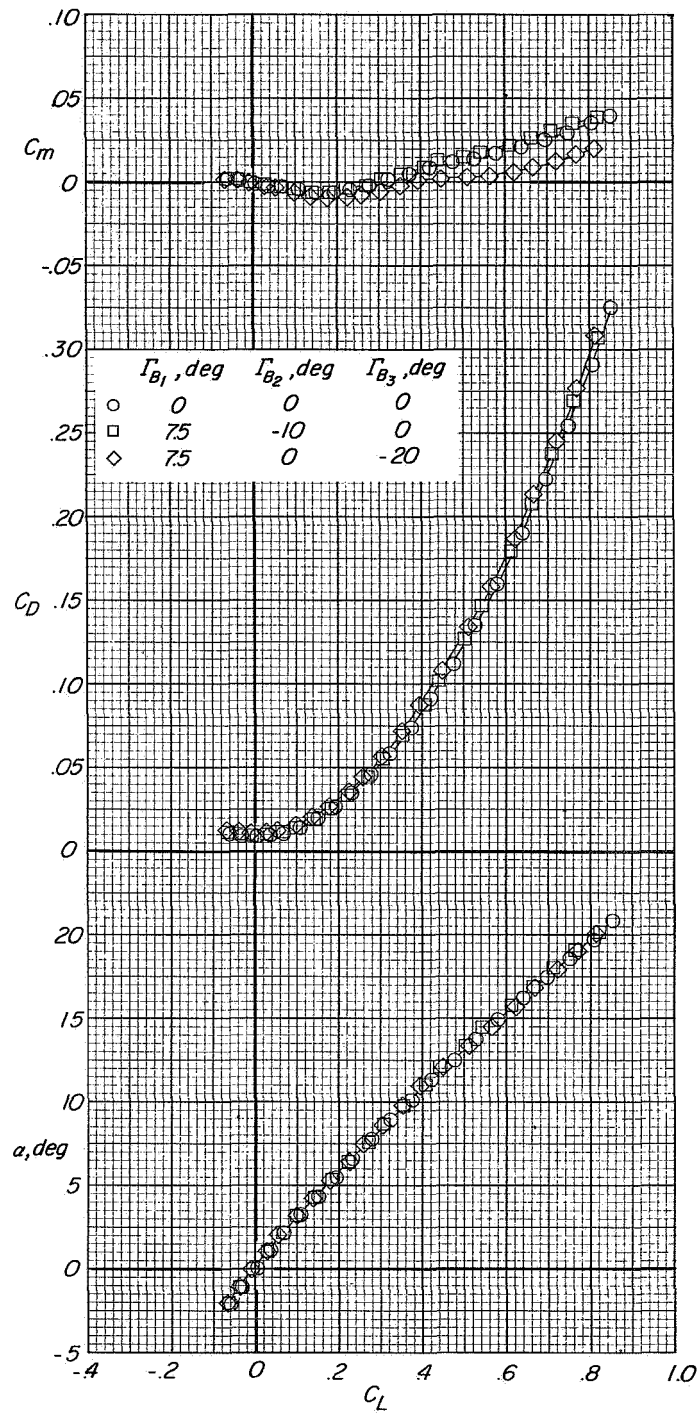
(c) Longitudinal characteristics;  $\Gamma_B = -20.0^\circ$  to  $10.0^\circ$ .

Figure 9.- Continued.



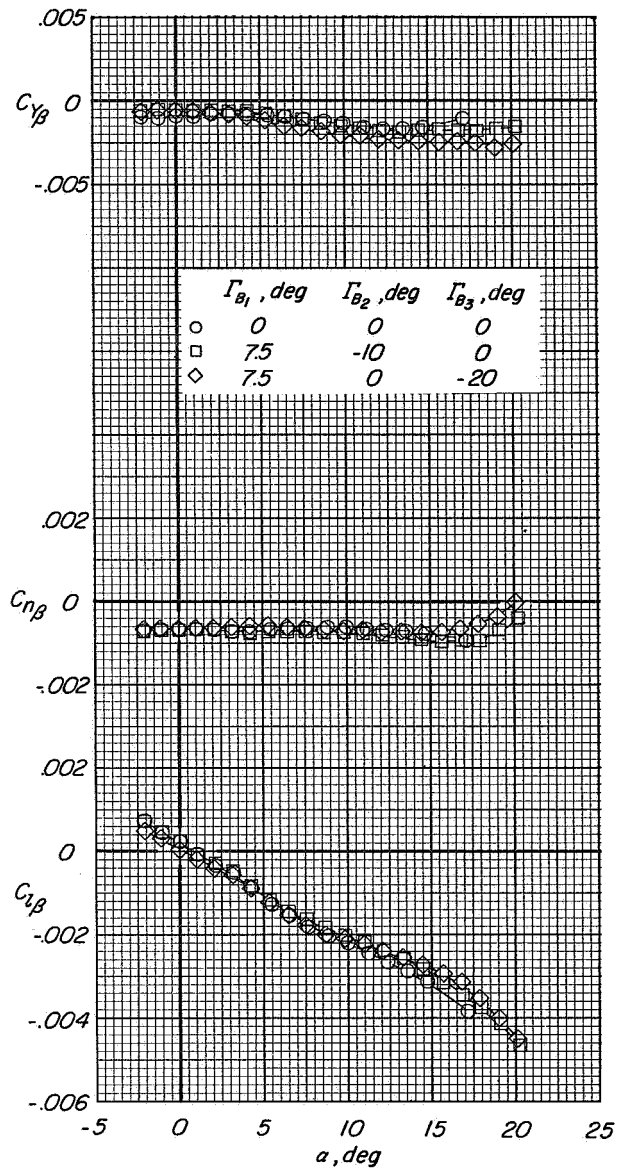
(d) Lateral directional characteristics;  $\Gamma_B = -20.0^\circ$  to  $10.0^\circ$ .

Figure 9.- Continued.



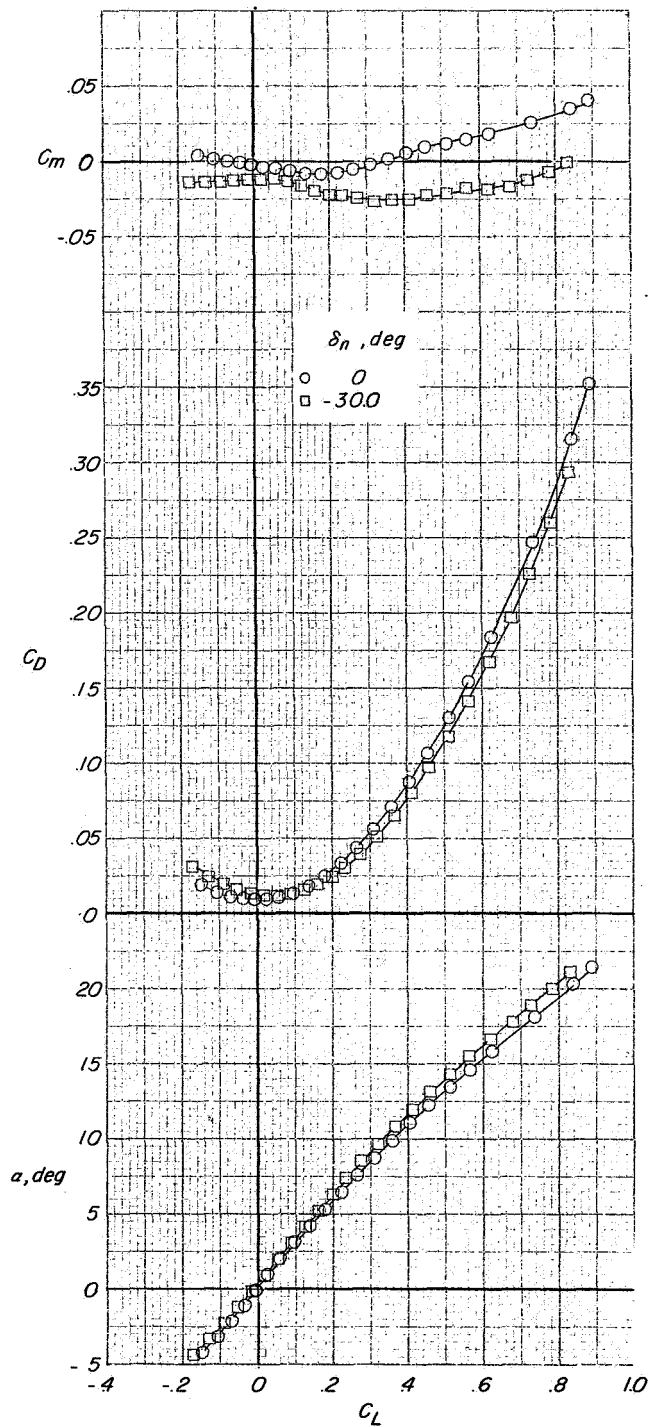
(e) Longitudinal characteristics;  $\Gamma_B = -20^\circ$  to  $7.5^\circ$ .

Figure 9.- Continued.



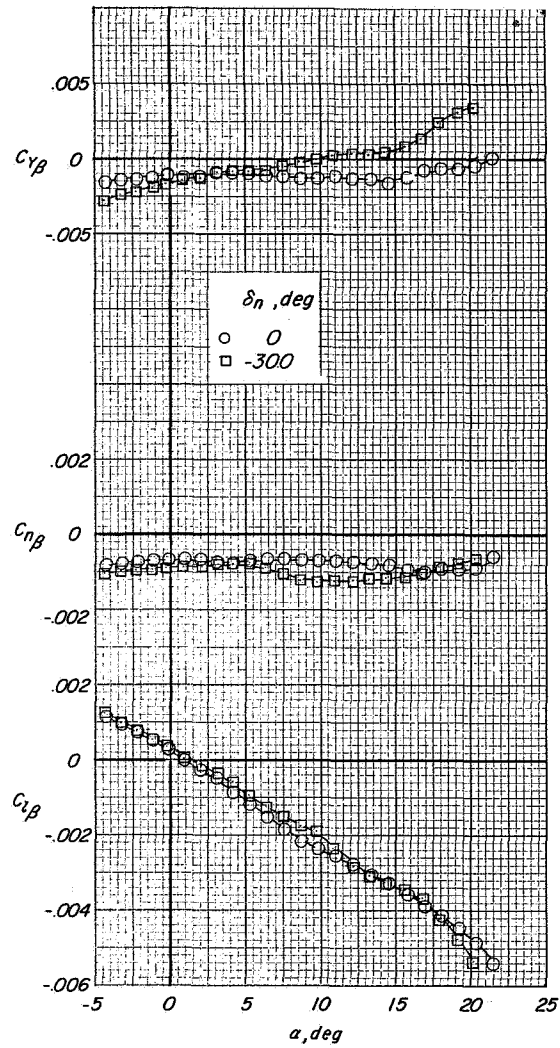
(f) Lateral directional characteristics;  $\Gamma_B = -20^\circ$  to  $7.5^\circ$ .

Figure 9.- Concluded.



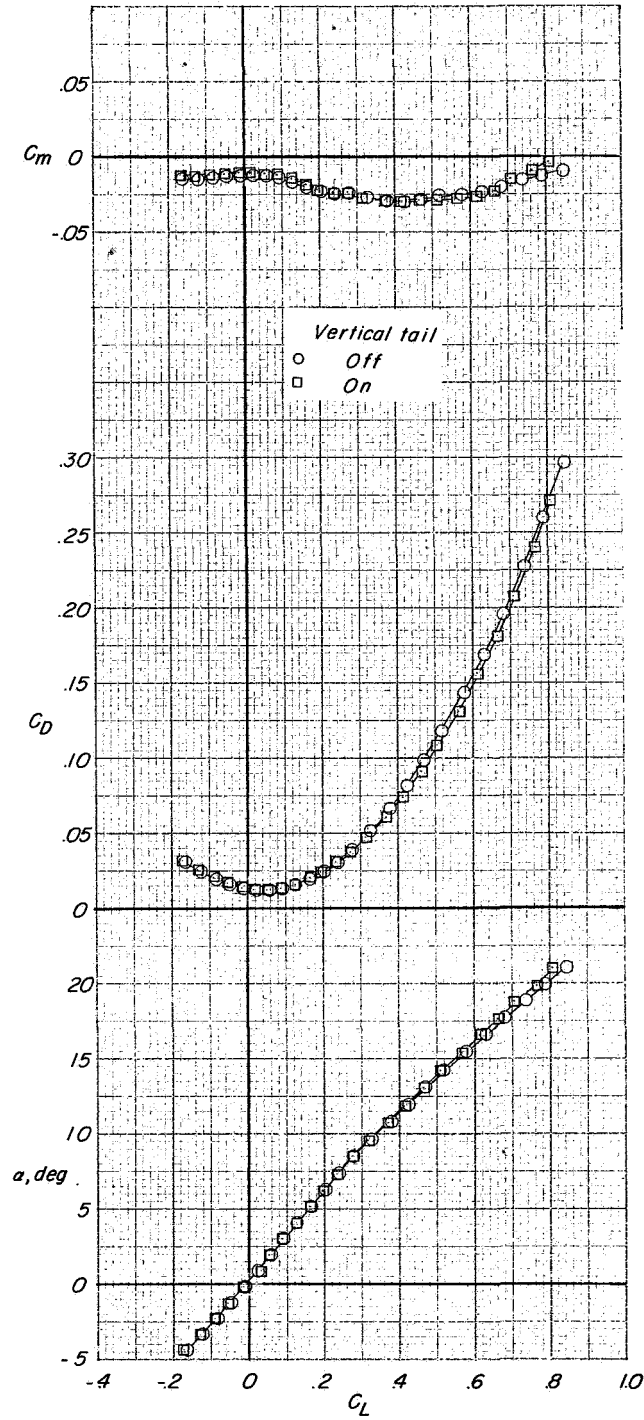
(a) Longitudinal characteristics.

Figure 10.- Effect of leading-edge flap deflection on aerodynamic characteristics.  $\Gamma_B = 0^\circ$ ;  $V_t$  off.



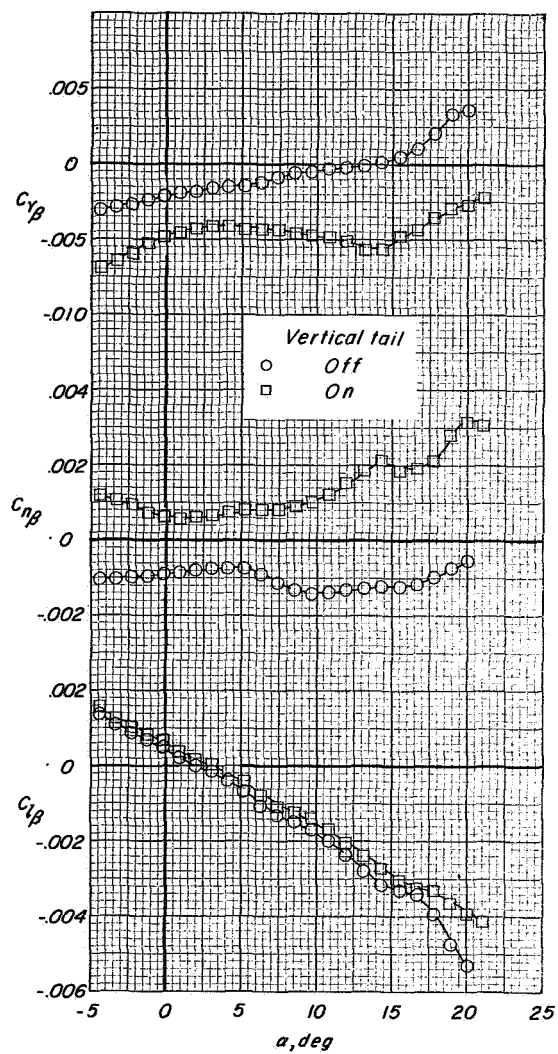
(b) Lateral directional characteristics.

Figure 10.- Concluded.



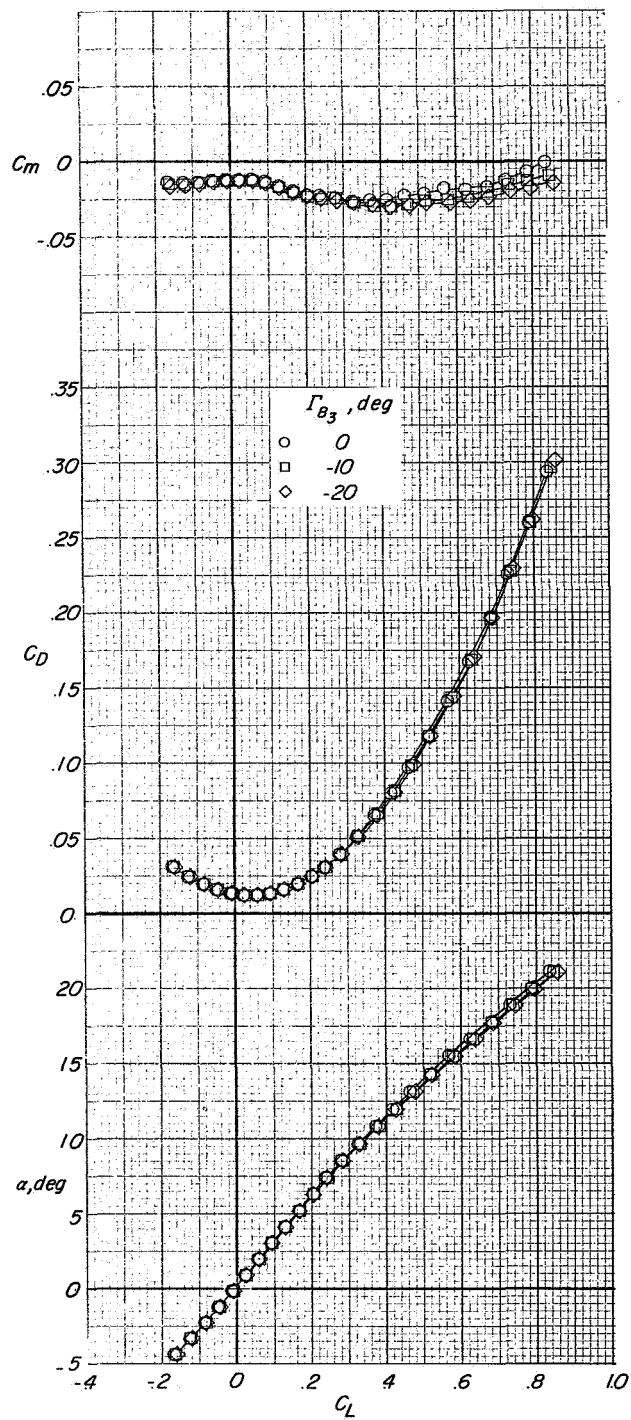
(a) Longitudinal characteristics.

Figure 11.- Effect of vertical tails on aerodynamic characteristics of configuration with leading-edge flap deflected  $-30^\circ$ .  
 $\Gamma_{B1} = 0^\circ$ ;  $\Gamma_{B2} = 0^\circ$ ;  $\Gamma_{B3} = -10^\circ$ .



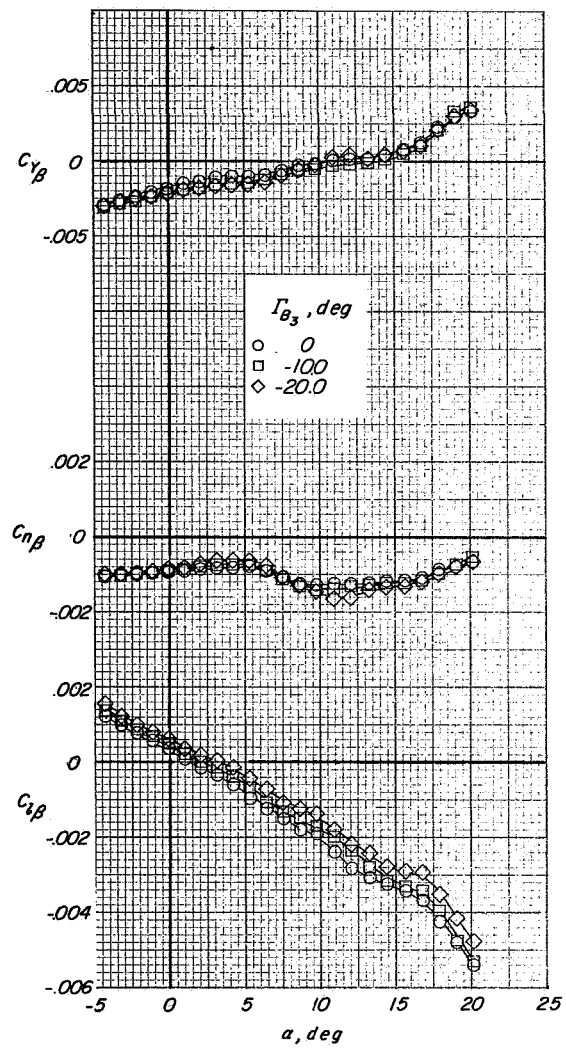
(b) Lateral directional characteristics.

Figure 11.- Concluded.



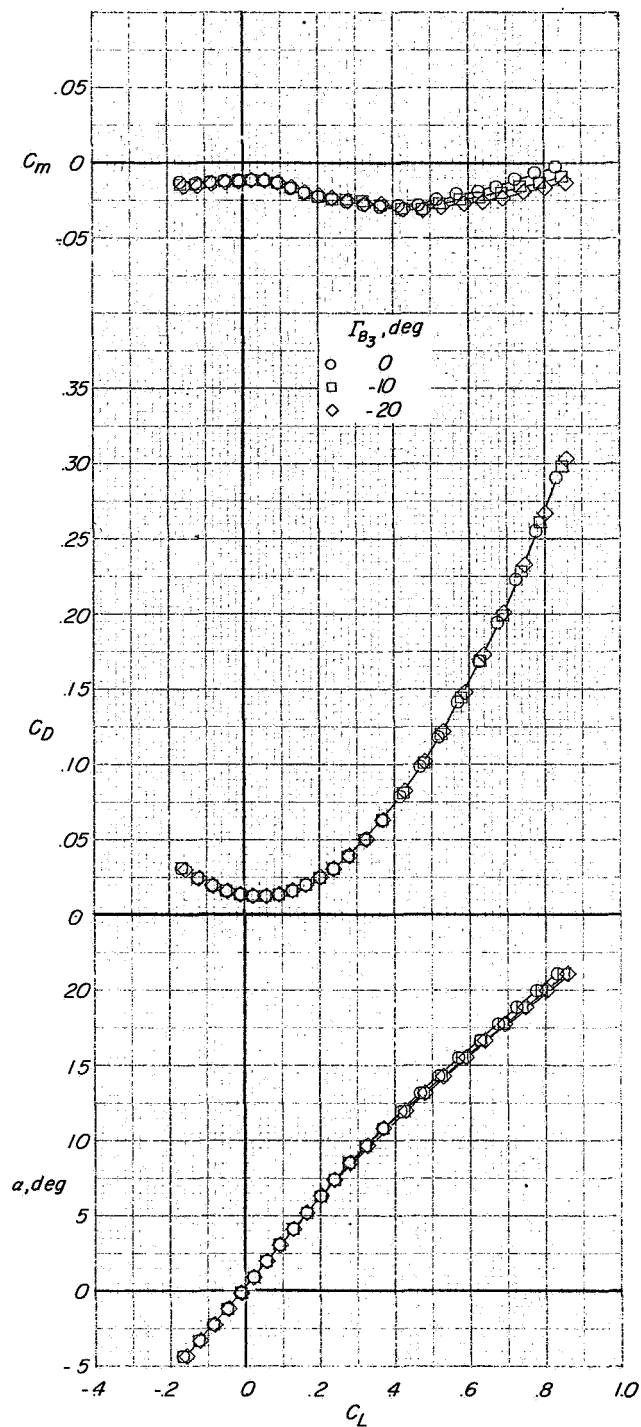
(a) Longitudinal characteristics.

Figure 12.- Effect of geometric dihedral at wing-break location 3 on aerodynamic characteristics.  $\Gamma_{B1} = 0^\circ$ ;  $\Gamma_{B2} = 0^\circ$ ;  $\delta_n = -30^\circ$ ;  $V_t$  off.



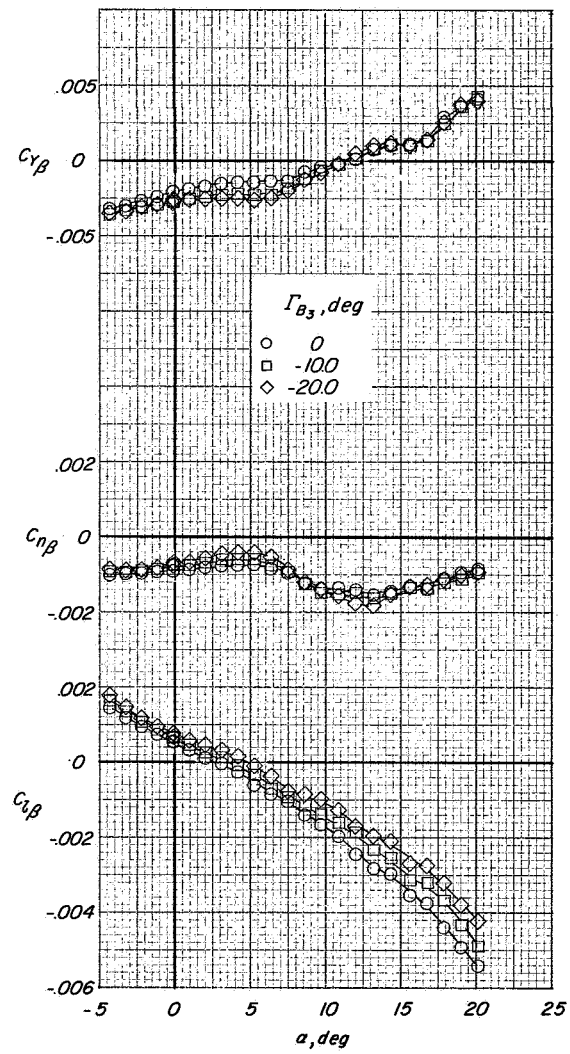
(b) Lateral directional characteristics.

Figure 12.- Concluded.



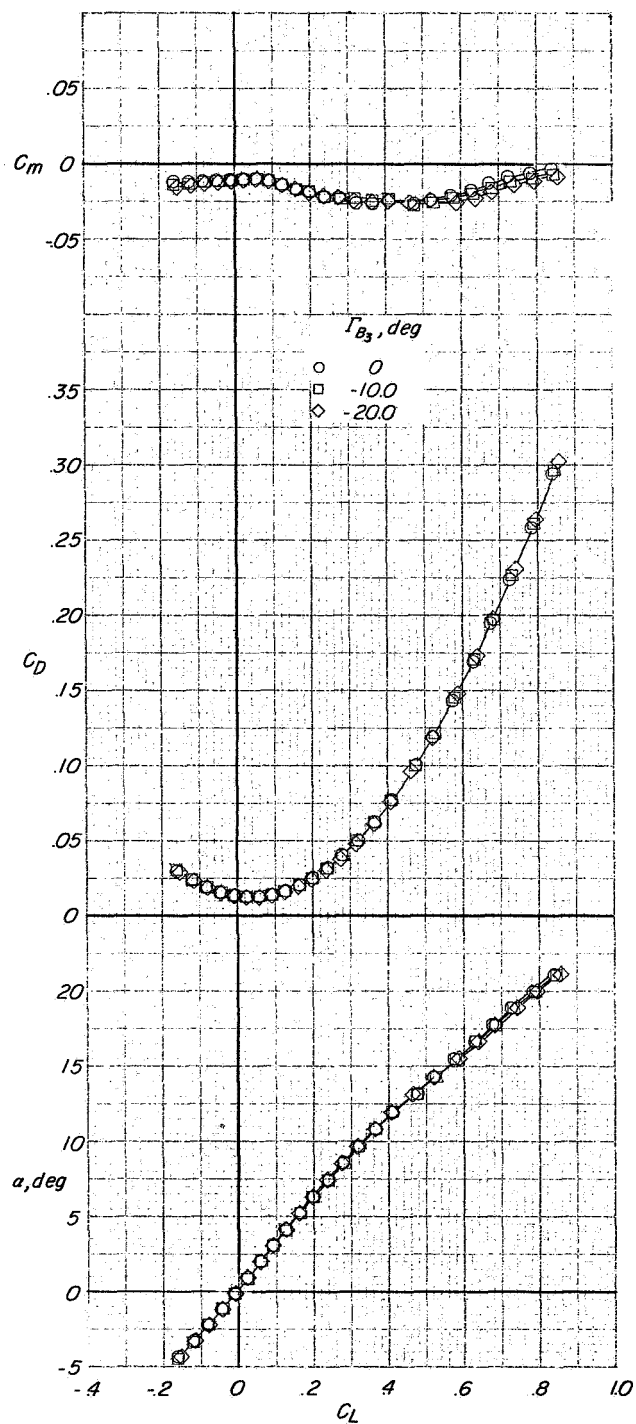
(a) Longitudinal characteristics.

Figure 13.- Effect of geometric dihedral at wing-break location 3 on aerodynamic characteristics.  $\Gamma_{B_1} = 0^\circ$ ;  $\Gamma_{B_2} = -5^\circ$ ;  $\delta_n = -30^\circ$ ;  $V_t$  off.



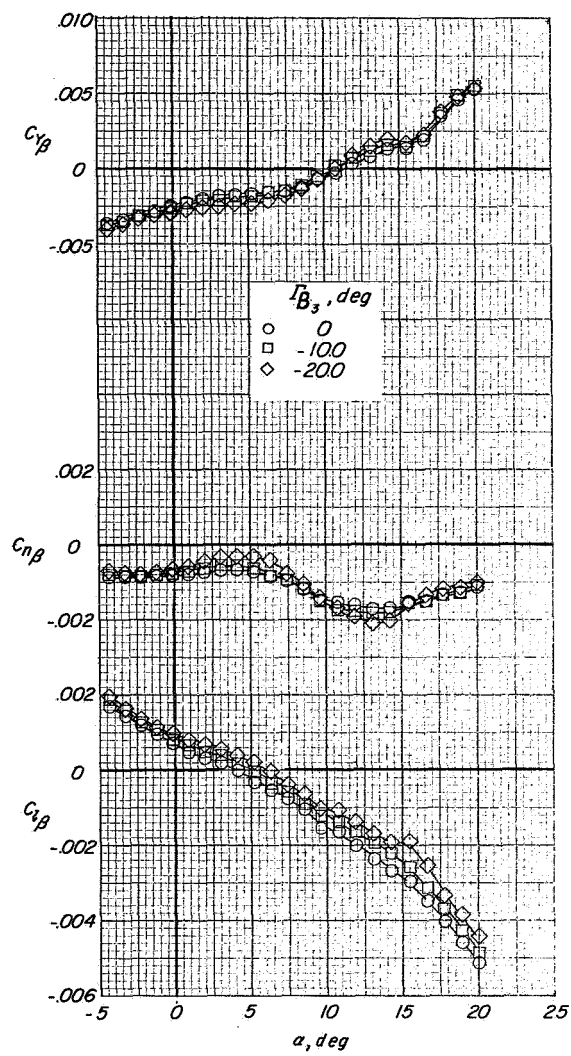
(b) Lateral directional characteristics.

Figure 13.- Concluded.



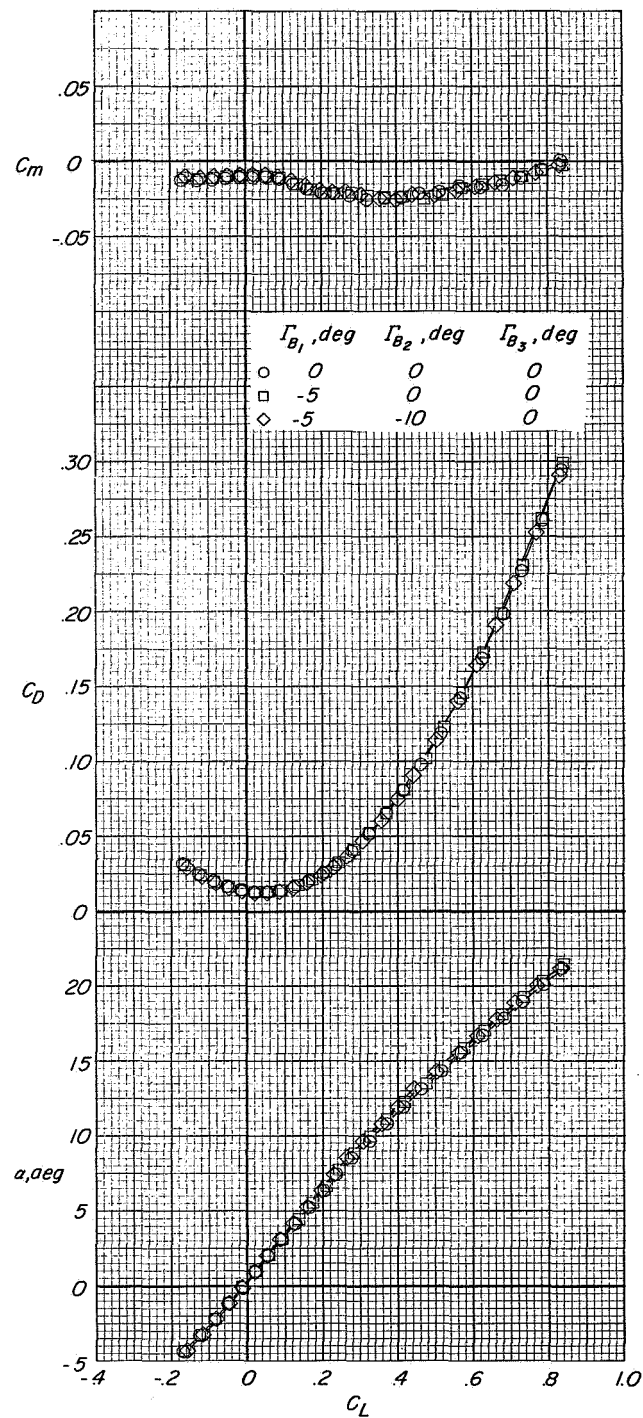
(a) Longitudinal characteristics.

Figure 14.- Effect of geometric dihedral at wing-break location 3 on aerodynamic characteristics.  $\Gamma_{B_1} = 0^\circ$ ;  $\Gamma_{B_2} = -10^\circ$ ;  $\delta_n = -30^\circ$ ;  $V_t$  off.



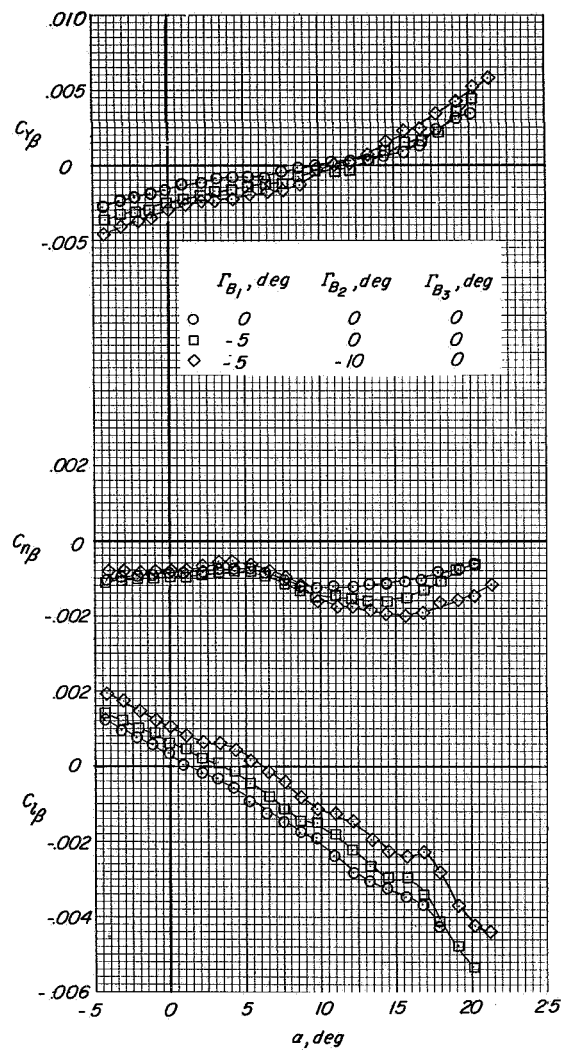
(b) Lateral directional characteristics.

Figure 14.- Concluded.



(a) Longitudinal characteristics.

Figure 15.- Effect of geometric dihedral on aerodynamic characteristics.  $\delta_n = -30^\circ$ ;  $V_t$  off.



(b) Lateral directional characteristics.

Figure 15.- Concluded.

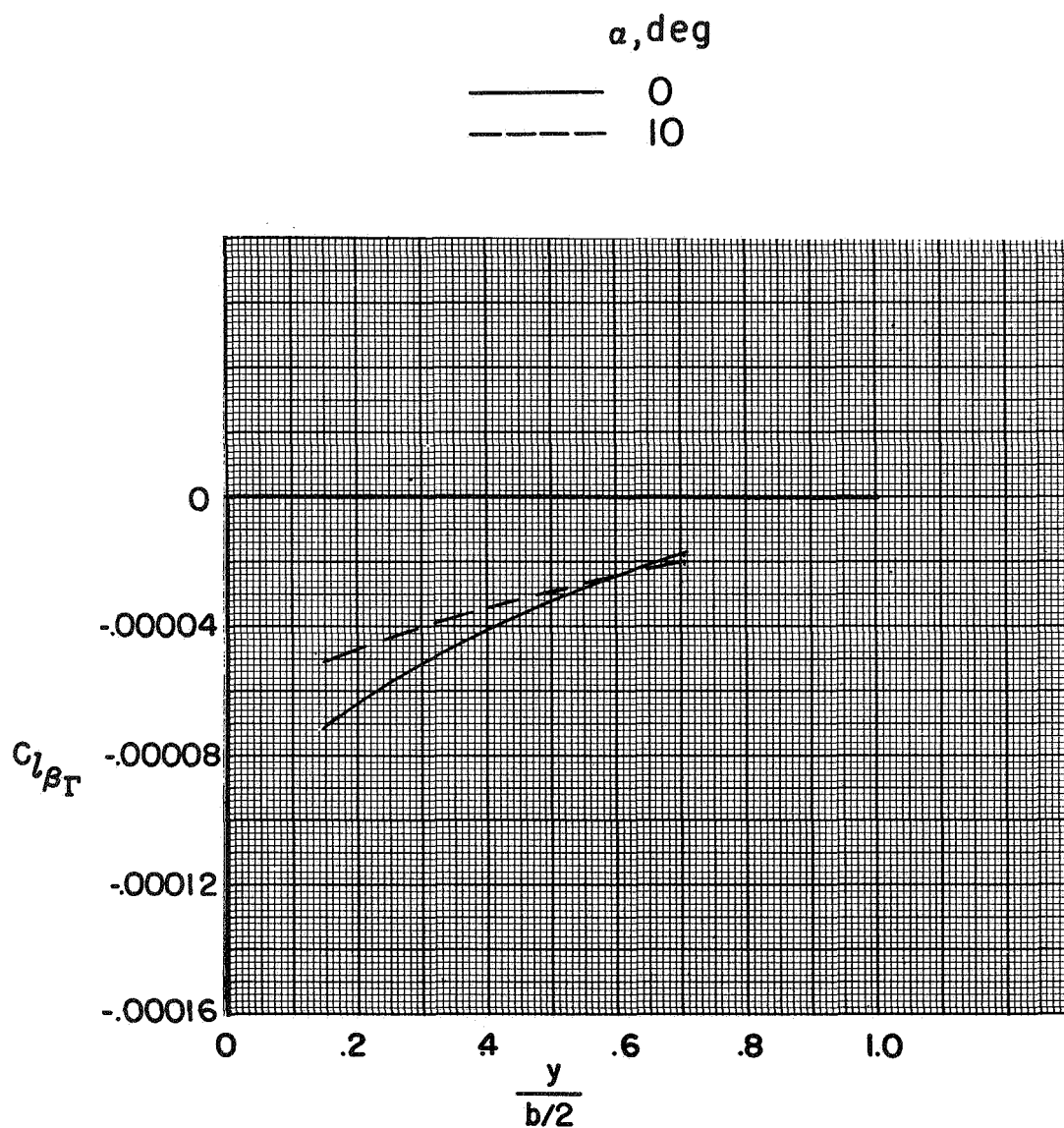


Figure 16.- Variation of effective-dihedral parameter with spanwise location of geometric-dihedral angle.

NATIONAL AERONAUTICS AND SPACE ADMINISTRATION  
WASHINGTON, D. C. 20546  
OFFICIAL BUSINESS  
PENALTY FOR PRIVATE USE \$300

FIRST CLASS MAIL



POSTAGE AND FEES PAID  
NATIONAL AERONAUTICS AND  
SPACE ADMINISTRATION

POSTMASTER: If Undeliverable (Section 158  
Postal Manual) Do Not Return

*"The aeronautical and space activities of the United States shall be conducted so as to contribute . . . to the expansion of human knowledge of phenomena in the atmosphere and space. The Administration shall provide for the widest practicable and appropriate dissemination of information concerning its activities and the results thereof."*

—NATIONAL AERONAUTICS AND SPACE ACT OF 1958

## NASA SCIENTIFIC AND TECHNICAL PUBLICATIONS

**TECHNICAL REPORTS:** Scientific and technical information considered important, complete, and a lasting contribution to existing knowledge.

**TECHNICAL NOTES:** Information less broad in scope but nevertheless of importance as a contribution to existing knowledge.

**TECHNICAL MEMORANDUMS:** Information receiving limited distribution because of preliminary data, security classification, or other reasons.

**CONTRACTOR REPORTS:** Scientific and technical information generated under a NASA contract or grant and considered an important contribution to existing knowledge.

**TECHNICAL TRANSLATIONS:** Information published in a foreign language considered to merit NASA distribution in English.

**SPECIAL PUBLICATIONS:** Information derived from or of value to NASA activities. Publications include conference proceedings, monographs, data compilations, handbooks, sourcebooks, and special bibliographies.

**TECHNOLOGY UTILIZATION PUBLICATIONS:** Information on technology used by NASA that may be of particular interest in commercial and other non-aerospace applications. Publications include Tech Briefs, Technology Utilization Reports and Technology Surveys.

*Details on the availability of these publications may be obtained from:*

**SCIENTIFIC AND TECHNICAL INFORMATION OFFICE**

**NATIONAL AERONAUTICS AND SPACE ADMINISTRATION**

Washington, D.C. 20546